Pollen-based reconstruction of Holocene land-cover in mountain regions: Evaluation of the Landscape Reconstruction Algorithm in the Vicdessos valley, northern Pyrenees, France

Laurent Marquer, Florence Mazier, Shinya Sugita, Didier Galop, Thomas Houet, Élodie Faure, Marie-José Gaillard, Sébastien Haunold, Nicolas de Munnik, Anaëlle Simonneau, et al.

Highlights

- Pollen-based reconstruction of Holocene land-cover in mountain regions
- The LRA approach is effective in mountain regions
- The REVEALS-based estimates are influenced by the systematic selection of pollen sites
- Pollen proportions alone are not useful for the local reconstruction
- New horizons for answering questions about human impact on upland vegetation

Pollen-based reconstruction of Holocene land-cover in mountain regions: evaluation of the Landscape Reconstruction Algorithm in the Vicdessos valley, Northern Pyrenees, France

Laurent Marquer [a,b,c*], Florence Mazier [b], Shinya Sugita [d], Didier Galop [b], Thomas Houet [e], Elodie Faure [b], Marie-José Gaillard [f], Sébastien Haunold [a,b], Nicolas de Munnik [b], Anaëlle Simonneau [g], François De Vleeschouwer [a,h], Gaël Le Roux [a]

[a] EcoLab (Laboratoire Ecologie Fonctionnelle et Environnement), ENSAT, UMR-CNRS 5245, Castanet Tolosan (France), laurent.marquer.es@gmail.com; francois.devleeschouwer@ensat.fr; gael.leroux@ensat.fr; sebastien.haunold@ensat.fr

[b] GEODE, UMR-CNRS 5602, Labex DRIIHM (OHM Pyrénées Haut Vicdessos), Université Toulouse Jean Jaurès (France), florence.mazier@univ-tlse2.fr; elo_faure@yahoo.fr; nicolas.demunnik@univ-tlse2.fr; didier.galop@univ-tlse2.fr

[c] Research Group for Terrestrial Palaeoclimates, Max Planck Institute for Chemistry, Mainz (Germany), l.marquer@mpic.de

[d] Institute of Ecology, Tallinn University (Estonia), sugita@tlu.ee

[e] LETG-Rennes COSTEL, UMR 6554 CNRS, Université Rennes 2 (France), thomas.houet@univ-rennes2.fr

[f] Department of Biology and Environmental Science, Linnaeus University (Sweden), marie-jose.gaillard-lemdahl@lnu.se

[g] OSUC, Observatoire des Sciences de l'Univers en région Centre, Université d'Orléans (France), anaelle.simonneau@univ-orleans.fr

[h] Instituto Franco-Argentino para el Estudio del Clima y sus Impactos (UMI IFAECI/CNRS-CONICET-UBA-IRD), Dpto. de Ciencias de la Atmosfera y los Oceanos, FCEN, Universidad de Buenos Aires, Argentina, fdevleeschouwer@cima.fcen.uba.ar

* Corresponding author:

Laurent Marquer

E-mail: laurent.marquer.es@gmail.com; l.marquer@mpic.de

ABSTRACT

Long-term perspectives on climate- and human-induced shifts in plant communities and tree line in mountains are often inferred from fossil pollen records. However, various factors, such as complex patterns of orographic wind fields and abundant insect-pollinated plants in higher altitudes, make pollen-based reconstruction in mountain regions difficult.

Over the last decade the Landscape Reconstruction Algorithm (LRA) - a model-based approach in reconstruction of vegetation – has been successfully applied in various parts of the globe. However, evaluation of its effectiveness in mountain ranges is still limited. The present study assesses the extent to which the LRA approach helps quantify the local changes in vegetation cover at Vicdessos valley in northern French Pyrenees as a case study. In the study area well-dated sediment cores are available from eight bogs and ponds, 6 – 113 m in radius, located above the current tree line. We first use a simple simulation experiment to evaluate the way how pollen records from "landscape islands" (mountain tops and plateaus) would represent local vegetation and to clarify important factors affecting the LRA-based reconstruction in a mountainous region. This study then uses pollen records from these sites and vegetation and land-cover data both within a 50-km radius around the Vicdessos valley and within a 2-km radius from each site for evaluation of the REVEALS- and LOVE-based reconstruction of the regional and local plant cover, respectively, in the LRA approach. The land-cover data are complied for coniferous trees, broadleaved trees and non-forested

areas from the CORINE and historical maps in three time windows: 1960-1970, 1990-2000 and 2000-2013.

Major findings are as follows. (1) Accuracy of the regional vegetation estimates affects the reliability of the LRA-based reconstruction of vegetation within a 2-km radius; use of the CORINE data as input to the LOVE model improves reliability of the results over the use of the REVEALS-based estimates of regional vegetation. This implies that a systematic selection of pollen data only from sites above the tree line is problematic for estimating regional vegetation, and thus the entire LRA process. (2) Selection of the dispersal models for pollen transport (i.e. the Langrangian Stochastic Model vs. Gaussian Plume Model) does not affect significantly the LRA-based estimates at both the regional and local scales in the study area. (3) The LRA approach improves the pollen-based reconstruction of local vegetation compared to pollen percentage alone in northern Pyrenees. Although further empirical and simulation studies are necessary, our results emphasize the importance of site selection for the LRA-based reconstruction of vegetation in mountain regions.

Keywords Vegetation, Land use, Landscape, Open land, REVEALS, LOVE, Holocene, France

1. INTRODUCTION

Mountain landscapes in Europe are expected to change significantly over the next few decades because of the ongoing climate change and reforestation caused by the abandonment of agro-pastoral areas (IPCC, 2014). These human-induced changes in climate and land cover will affect undoubtedly species composition and spatial dynamics of plant communities on mountains, including altitudinal shifts in tree lines (Leunda et al., 2019). All those expected changes in mountain regions will impact on a large range of ecosystem services, including tourism, recreation, water resources (Szczypta et al., 2015) and loss of traditional land-use.

The Pyrenean mountains have been under intense human influence (e.g. pastoralism and deforestation) since the Bronze Age (Galop et al., 2013) and have undergone major transformations during the last century. Owing to rural depopulation, traditional pastoral management has declined since the 1950s (MacDonald et al., 2000). The history of the Vicdessos area in northeastern Pyrenees is closely related to this progressive depopulation and the associated abandonment of former management practices. This has led to fast reforestation of the slopes and replacement of pastoral uplands by forests and heathlands (Houet et al., 2012, 2015; Vacquié et al., 2016), as in many European mountains (Kozak et al., 2017). This has further resulted in a loss of plant diversity (Galop et al., 2011) and insect species richness (e.g. hoverflies) in an adjacent valley (Herrault et al., 2016). Those baseline information on the past mountain landscapes are critical to evaluate the effects of

current and future land-use changes on high altitude ecosystems, biodiversity and for sustainable land-management strategies.

Fossil pollen records have provided information on the century- to millennium-scale changes in the past land cover. However, interpretation of pollen data is tricky in mountain regions because of the complex physical and biological conditions and factors that influence the pollen-vegetation relationships in unknown ways (e.g. Ortu et al., 2006; Leunda et al., 2017; Zhang et al., 2017). There are several possible reasons: 1) The amount of long-distance pollen, particularly arboreal pollen types from lower altitudes brought by orographic wind, overwhelms local pollen signals of meadows and parklands in alpine zones (Markgraf, 1980; Randall, 1990; Fall, 1992; David, 1993, 1997; Ortu et al., 2006; Zhang et al., 2017). 2) Plant communities vary significantly within relatively short distances along mountain slopes and altitudes; accordingly, pollen records from mountain sites tend to reflect several vegetation types together that are closely located (Fall, 1992). 3) Differences in plant phenology between mountains and lowlands, especially flowering timing of plants of the same species, make interpretation of pollen records difficult (Fall, 1992; Leunda et al., 2017). 4) Insect-pollinated plants - the dominant type of plants in alpine zones - tend to be low pollen-producers, thus biasing pollen representation of vegetation (Markgraf, 1980; Fall, 1992). 5) Wind gradients and directions are often site-specific in mountains, thus it is difficult to generalize what pollen records represent (Markgraf, 1980). To reduce the uncertainties associated with these issues, palaeoecologists

105 often use both macro-remains of plants and pollen for reconstruction of the local- to landscape-scale
106 changes in mountain plant communities (e.g. Birks and Birks, 2000; Leunda et al., in press).

107 The present study aims to explore applicability of modeling approaches that overcome some
108 of these difficult issues and evaluate the extent to which models help to improve the interpretation of
109 pollen records in mountain regions. In the next section we first explore feasibility of the Landscape
110 Reconstruction Algorithm (LRA; Sugita, 2007a, 2007b) – a two-step model-based reconstruction
111 approach – for mountain vegetation, using simple simulations based on the POLLSCAPE models
112 (e.g., Sugita 1994; Broström et al., 2005; Gaillard et al., 2008; Hjelle and Sugita, 2012). The LRA
113 has been used widely in many parts of Europe and elsewhere over the last decade with a reasonable
114 success, especially in relatively flat and less complex geomorphological terrains. We create simplified
115 simulated landscapes that represent mountain landscapes on a two-dimensional space, and then
116 evaluate the potential and limitations of the LRA approach in the idealized simulated situations. With
117 insights into the LRA applicability from the simulations at hand, the rest of this paper evaluates
118 empirically the applicability and reliability of the LRA approach around the Vicdessos valley in the
119 Pyrenees. The study area is well suited for this study, because (1) well-dated pollen records from
120 eight sites are available at and above the tree line, and (2) the regional- and local-scale land-cover
121 maps are available in three time periods (i.e., 1960-1970, 1990-2000 and 2000-2013) for comparison
122 with the pollen-based reconstruction of the past land cover. Major assumptions and current important

123 issues related to the LRA are described in detail in the method section, Appendix A and wherever
124 appropriate. We then discuss pros and cons of the LRA-based reconstruction in mountains and
125 address future directions to improve the approach.
126
127 **2. FEASIBILITY OF LRA-BASED RECONSTRUCTION OF VEGETATION IN**
128 **MOUNTAIN REGIONS: EVALUATION WITH SIMULATED LANDSCAPES**
129 Besides the complex nature of the wind field on mountains and juxtaposition of plant
130 communities within short distances along short elevational gradients, a systematic selection of sites
131 restricted only to mountain tops and plateaus also potentially biases pollen representation of
132 vegetation, thus affecting the accuracy of the LRA. It is a common practice to select pollen sites
133 located only in sub-alpine or alpine zones because of the availability of sediments free from human-
134 related disturbances (Simonneau et al., 2013). This site-selection scheme would influence the
135 evaluation of long-distance pollen from lower altitudes - an important step for objective
136 reconstruction of local vegetation on mountains (Sugita, 2007a,b).
137 The current section uses the POLLSCAPE approach (*sensu* Sugita, 2013) to evaluate the
138 extent to which this site-selection scheme would affect the entire LRA process. In the POLLSCAPE
139 simulations we regard mountain tops and high-altitude plateaus as "landscape islands" on a flat two-
140 dimensional terrain, 80 km x 80 km in size, for the sake of simplicity (as in Sugita, 1994; Sugita et

141 al., 1997, 1999; Bunting et al., 2004; Broström et al., 2004, 2005; Gaillard et al., 2008; Hjelle and
142 Sugita, 2012). Although generalized, the simulated landscapes depict the characteristics of the spatial
143 structure and species composition of plant communities in high-altitude plateaus and the regional
144 vegetation around the Vicdessos valley (see section 3.1.). Figure 1a illustrates the general scheme of
145 the simulated landscapes with randomly located patches of specific plant-community types within
146 the Matrix. Seven plant/pollen types are included for simulations: *Betula*, *Calluna*, Ericaceae, *Fagus*,
147 *Quercus*, Poaceae and *Pinus*. The Matrix and Patch Type B represent plant communities in lower
148 altitudes in mountain valleys and flat plains, characterized by forests of mixed broadleaved and
149 conifer trees (*Fagus*, *Quercus* and *Pinus*) and grass (Poaceae)-dominated open areas, respectively.
150 Patch Type A symbolizes mountain tops that are characterized by Ericaceae plants (including
151 *Rhododendron* spp. and *Vaccinium* spp.) with semi-dominant grass and *Calluna* (heather). In Patch
152 Type A, small-patches of two types of heather heathlands are placed to fine-tune the local spatial
153 structure of vegetation: Patch Type C with heather, grass and Ericaceae and Patch Type D with
154 heather, grass, Ericaceae and *Pinus*.

155 The LRA consists of two steps: the first to estimate regional vegetation within <50-100 km
156 with the REVEALS model and the second to reconstruct the local- and landscape-scale changes in
157 vegetation within the relevant source area of pollen (RSAP; *sensu* Sugita, 1994). Each step requires
158 pollen counts from multiple sites that are ideally selected randomly within the targeted area of interest.

159 For either REVEALS or LOVE calculation, one of the patches of Patch Type A is selected randomly
160 in the central part of the plot, and a lake is placed within the area of the patch. For REVEALS
161 applications a lake 500-m in radius is placed at the center of the patch selected, and for LOVE
162 applications a lake 50-m in radius is located randomly within the patch. In each simulation run, we
163 repeat this process thirty times to obtain pollen counts from 30 lakes for REVEALS and LOVE,
164 separately. Pollen loading on lakes, with which pollen counts are simulated, is calculated by Sugita's
165 model for pollen deposition on lakes (Sugita, 1993). Pollen transport in air is approximated by both
166 a Gaussian Plume model (GPM) (Prentice, 1985; Sugita, 1993, 1994, 2007a, 2007b) and a Lagrangian
167 Stochastic model (LSM) of Kuparinen et al. (2007) and Theuerkauf et al. (2013, 2016). Pollen
168 productivity estimates – important parameters for the pollen loading calculation – are after Mazier et
169 al. (2012). We assume that the simulated pollen records are independently obtained at each site. These
170 records are used as inputs for the LRA-based reconstruction of vegetation around each site. The
171 LOVE results are expressed as area proportions within the RSAP for three categories: conifers (i.e.
172 *Pinus*), broadleaved trees (i.e. *Betula*, *Quercus* and *Fagus*) and open land (i.e. Poaceae, *Calluna* and
173 Ericaceae); by definition all the LOVE results are expressed in a distance-weighted fashion (Distance
174 Weighted Plant Abundance: DWPA) (Sugita, 2007b; Sugita et al., 2010). Appendix A provides a
175 brief description and sets of parameters necessary for the POLLSCAPE simulations and the LRA
176 calculation.

177 Figure 1b shows the LRA results against the DWPA of the three land-cover categories within
178 the RSAP. The LRA approach improves the accuracy of vegetation reconstruction significantly over
179 the pollen proportions alone. Considering the standard errors, the reconstructed values are not
180 significantly different from the 1:1 line along the two axes. Note that the standard errors of the open
181 land category are large, suggesting large uncertainties to be expected in reconstruction of the local
182 open land. The selection of the different dispersal models of pollen did not cause large differences in
183 the LRA-based reconstruction of the local vegetation. The inverse modelling of LOVE (Sugita,
184 2007b; Sugita et al., 2010) demonstrates that the RSAP is consistent in the simulations regardless of
185 the pollen dispersal models employed; the RSAP is within 310 m and 325 m with the GPM and LSM
186 options, respectively. With the LSM option, the variation in vegetation reconstruction among sites,
187 as well as the standard error estimate at each site, appears larger than that with the GPM option for
188 the three categories of land cover.
189

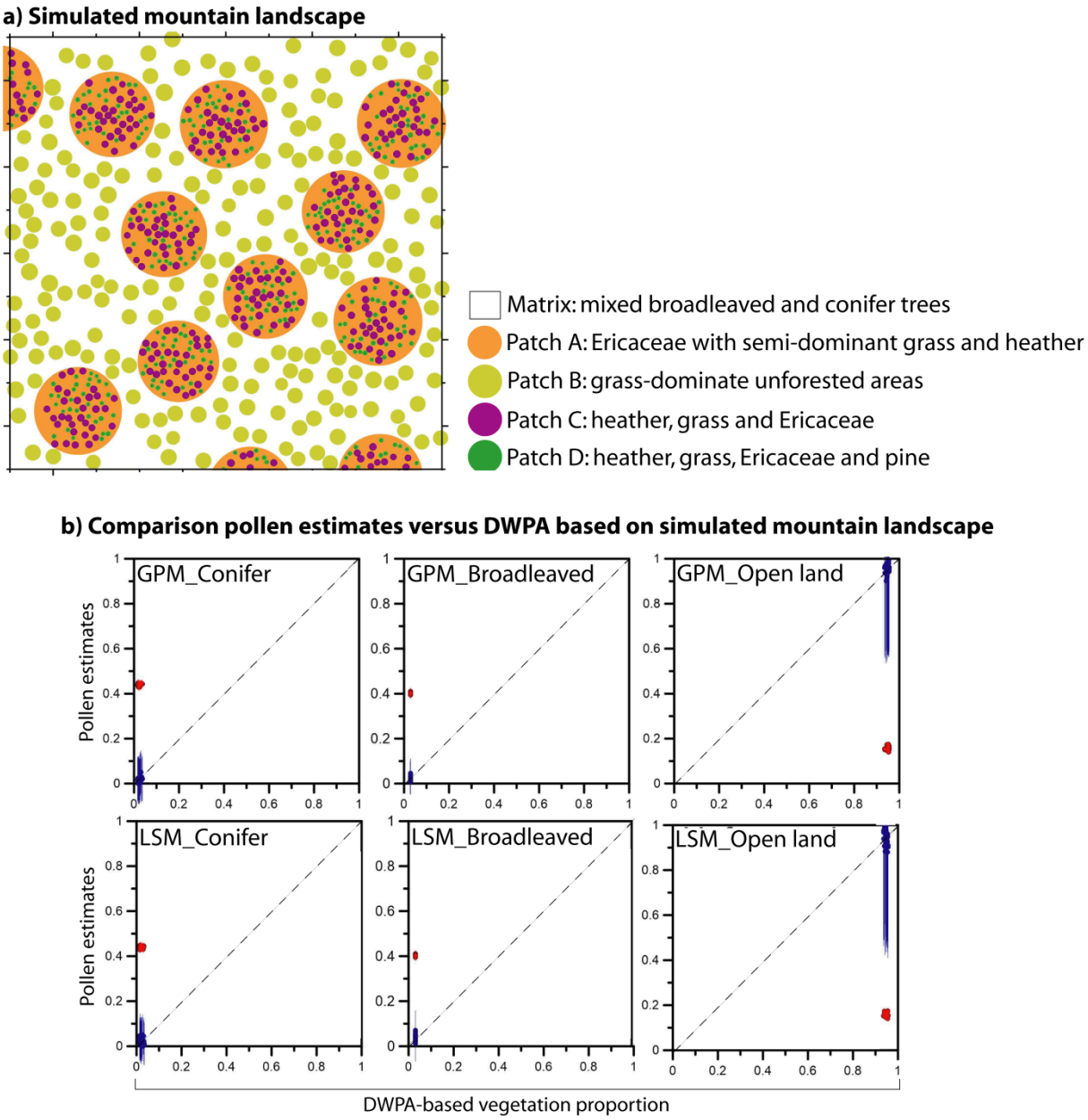

Figure 1a) Simulated mountain landscape that mimics the one of the Vicdessos valley to estimate pollen loadings on 30 lakes systematically located on mountain tops and plateaus. Mountain tops and plateaus correspond to Patch type A that includes two small patch types (Patch types C and D) of heather heathlands. The Matrix and Patch type B represent plant communities in lower altitudes in mountain valleys and flat plains. The simulated study plot is of 80 km x 80 km. More details about the simulation are given in the text and Appendix A. **b)** Results of LRA comparing distance weighted plant abundance (DWPA) based on observed vegetation (i.e. landscape design around each lake) against pollen proportion (untransformed pollen data; red dots) and two sets of LRA estimates (blue dots), one using GPM and the other LSM as pollen dispersal model. Each point represents a pollen record from each lake. Pollen proportion and LRA estimates are reasonable representation of observed vegetation when pollen records are close to the dashed line. Standard errors are also shown.

202 The simulation results provide insights into, and caveats for, pollen-based reconstruction of
203 vegetation in mountain regions such as in the Pyrenees.
204 (1) Accuracy of the regional estimates of vegetation and land cover matters for reliable LRA
205 applications in mountains as in any other regions. Ideally, the REVEALS application requires pollen
206 records from randomly-selected sites >100 ha in both mountains and lowland areas in the region of
207 interest. It is hard to achieve this scenario in reality, however. The simulation results suggest that, as
208 long as multiple pollen sites are available, the application of REVEALS and LOVE appears to provide
209 reasonable estimates of the regional and local vegetation even if the sites are systematically selected
210 only in the "mountain patches". Of course, large sites (e.g. 500 m in radius – ca. 78 ha – in the
211 simulations) would be preferable to reduce biases and uncertainties of the REVEALS results (Figure
212 1b); if only small sites 50 m in radius are used, we expect larger uncertainties for the regional
213 estimates, resulting in less reliable LRA outcomes (Appendix A).
214 (2) Differences in the LRA results between using the GMP and LSM as a pollen dispersal
215 model appear negligible in the simulation runs. Recent studies have shown that the LSM option
216 produces more realistic results in REVEALS-based reconstruction of regional vegetation, especially
217 for plants with heavy and light pollen types (Theuerkauf et al., 2013, 2016; Mariani et al., 2017) than
218 the GPM option does. Considering more advanced understanding of wind field and particle transport
219 in air (Kuparinen et al. 2007), the LSM option has advantages over the GPM option, especially for

220 describing long-distance pollen from regional sources. As the simulation results (Figure 1b) suggest,
221 however, consistency in dispersal-model selection for REVEALS and LOVE in the LRA process
222 helps provide robust LRA estimates for reconstruction of the local- to landscape-scale vegetation in
223 spatially and topographically complex terrains (e.g. Hjelle et al., 2015).
224
225 **3. MATERIALS AND METHODS**
226 **3.1 Geographical setting, site characteristics and pollen data collection**
227 We use pollen records from eight small sites: three lakes and five bogs (Table 1, Fig. 2)
228 situated between 1600 and 2000 m a.s.l. Seven sites are located on the plateau of Bassiès (Fig. 2) and
229 one site (ARBU) 6 km to the north. ARBU belongs to another small watershed that is also part of the
230 Vicdessos area. All sites are small, varying from 6 to 40 m in radius for bogs and from 60 to 113 m
231 in radius for lakes (Table 1).
232 Mean annual temperature in this area (over the 2000–2012 period) is around 7°C and mean
233 annual precipitation about 1640 mm (Quintana-Seguí et al., 2008). Snow season generally starts in
234 November/December and ends in April/May. Winds are mostly coming from the west and north-
235 west; wind speed varies from 0 to 4 $m.s^{-1}$ (Szczypta et al., 2015; Claustres, 2016).
236
237

Table 1 Metadata of the pollen archives.

Site name	Lat.DD	Long.DD	Elevation (m)	Site radius (m)	Basin type	Age/depth model and dating
Sigriou (SIG)	42.754	1.422	2000	66	Lake	Simonneau et al. (2013)
Legunabens (LEG)	42.764	1.431	1680	58	Lake	Appendix B
Arbu (ARBU)	42.821	1.437	1740	113	Lake	Appendix B
Escale (ESC)	42.761	1.430	1630	40	Bog	Hansson et al. (2017)
Fouzes (FOUZ)	42.766	1.410	1720	13	Bog	Appendix B
W1652a (W1652)	42.763	1.416	1660	6	Bog	Hansson et al. (2017)
Etang Mort (EM)	42.766	1.419	1670	36	Bog	Hansson et al. (2017)
Orry de Théo (OT)	42.766	1.415	1680	31	Bog	Galop et al. (2011)

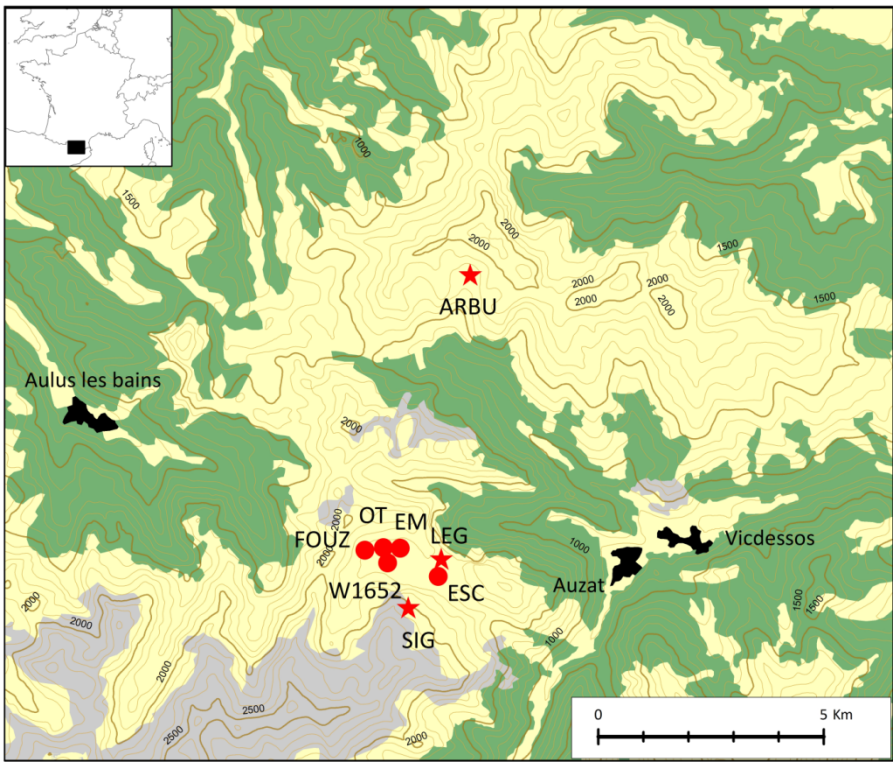

Figure 2 Location of the study area and pollen archives in the Vicdessos area (French Pyrenees). Yellow color corresponds to open land (above the tree line), green to forests and grey to mineral surfaces. Isolines of 100 m are shown. Seven pollen records (SIG, ESC, LEG, W1652, FOUZ, OT and EM) are located on the plateau of Bassiès and one (ARBU) 6km north of Bassiès (see Table 1 for the labels of the sites). Red dots are bogs and red stars are lakes.

246 Raw radiocarbon dates, dated materials and details on the age-depth models at individual sites
247 are given in Appendix B. Age-depth models of sediments are constructed by using both ^{210}Pb CRS
248 (Constant Rate of Supply) model (Appleby, 2002) and CLAM radiocarbon age depth model (Blaauw,
249 2010). In order to build a robust age-depth model at each site, uncertainties of the ^{210}Pb ages
250 calculated using Matlab with Monte Carlo simulations according to Binford (1990) are combined
251 with the radiocarbon uncertainties in CLAM. The pollen counts are pooled together for each 10-year
252 time window between 1960 and 2013; the most recent time window is 2000-2013. For this study we
253 select three time windows to assess the accuracy of the LRA-based reconstruction of vegetation:
254 1960-1970, 1990-2000 and 2000-2013; those are the time windows for which both the regional and
255 local land-cover maps are available. Total sum of pollen counts used for data analysis varies from
256 463 (SIG) to 2164 (FOUZ), 544 (EM) to 2530 (W1652), and 1143 (ARBU) to 5812 (OT) for the
257 periods 1960-1970, 1990-2000 and 2000-2013, respectively.
258
259 **3.2 Observed land-cover maps**
260 For evaluation of the LRA estimates, this study obtains the regional- and local/landscape-
261 scale estimates of plant composition for the areas within a 50-km radius from the plateau of Bassiès
262 and within a ca. 2-km radius from each site, respectively.
263

264 *3.2.1 Observed regional land-cover*

265 The CORINE Land Cover raster-based data (https://www.eea.europa.eu/data-and-maps/data)
266 for 1990 and 2006 are selected as a source of the observed regional land-cover for time windows of
267 1990-2000 and 2000-2013 (Fig. 3). The digitized vegetation map of Foix (oeuvre collective CNRS,
268 77 Foix, 1964, Henry Gaussen) in 1964 is used for the time window 1960-1970 (Fig. 3). Note that
269 this 1964 vegetation map does not cover the entire area in the 50-km radius. For this study the land-
270 cover maps from three time windows (1964, 1990 and 2006) are harmonized to be comparable to
271 each other.

272 The regional land-cover in 2006 is characterized by broadleaved forest (27%) and conifer
273 forest (16%) and grasslands (24%); arable and agricultural lands (12%) are mainly located in the
274 northernmost corner (Fig. 3). Oak and beech are the main components of the broadleaved forests,
275 associated with birch, hazel, lime-tree, willow and ash. Pine and fir characterize the conifer forests.
276 Forested areas have increased in the 1964-2013 period.

277

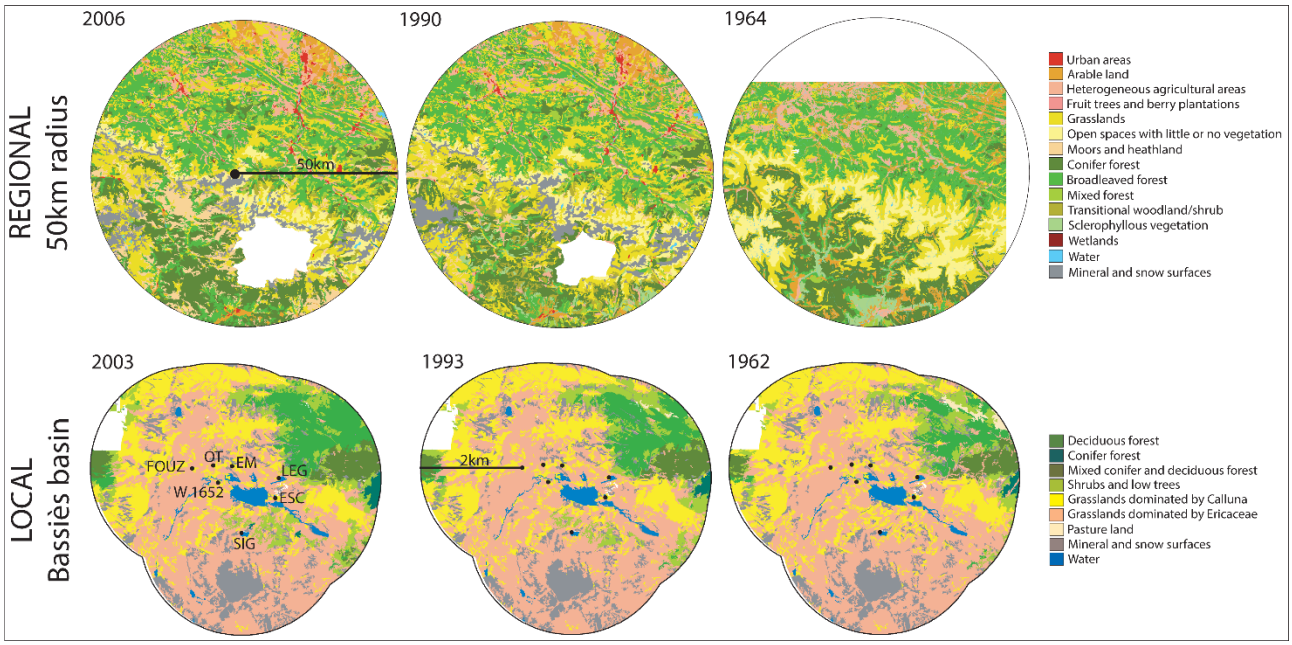

Figure 3 Observed regional land-cover maps of a 50-km radius from the plateaus of Bassiès and local land-cover maps of an agglomerated 2-km radius around each lakes and bogs (pollen archives). Regional maps are based on CORINE datasets for 2006 and 1990 and from the CNRS vegetation map "Foix 1964" for 1964. Local maps are based on series of aerial imageries (Houet et al., 2012). The meanings of the labels of each pollen record are given in Table 1. Note that white color corresponds to the absence of data.

3.2.2 Observed local land-cover

Local land-cover maps of the plateaus of Bassiès, which were compiled and created for 1962, 1993 and 2003 (Fig. 3), are suitable for the data-model comparison in the three time windows of our interest: 1960-1970, 1990-2000 and 2000-2013. These maps are based on a semi-automatic geographic object-based image analysis technique and visual interpretation of airborne imageries (Houet et al., 2012).

The plateaus of Bassiès is covered by heather and rhododendron heathlands and grasslands. Small clumps of short conifer trees are spread out over the plateaus unevenly. Forested areas are

293 located on the neighboring slopes; conifer trees are mostly pine and fir, and broadleaved trees mostly
294 beech, birch and hazel.
295
296 *3.2.3 Plant composition in individual land-cover types of the maps*
297 Twenty major plant/pollen types (Table 2), which are well presented in both the pollen records
298 and land-cover maps in the study region, are selected for data analysis. Plant composition in each
299 land-cover type is approximated according to a local botanical expert (N. de Munnik, personal
300 communication) and botanical survey on the plateaus of Bassiès (S. Haunold, unpublished). Details
301 about the plant composition in each land-cover type are given in Appendix C.
302
303
304
305
306
307
308
309 **Table 2** Taxa and groups of taxa used in this study. Relative pollen productivity estimates (RPPs) of individual taxa and
310 their standard errors, and fall speed of pollen are listed. RPP values are relative to that of Gramineae. Botanical
311 nomenclature follows *Flora Europaea* (Tutin et al., 1964-1980).
312

Pollen taxa	RPP and standard errors	Fall speeds of pollen (m/s)	Groups of taxa
Abies	6.88 +/- 1.44	0.12	Conifer trees
Juniperus	2.07 +/- 0.04	0.016	
Picea	2.62 +/- 0.12	0.056	
Pinus	6.38 +/- 0.45	0.031	
Betula	3.09 +/- 0.27	0.024	Broadleaved trees
Corylus	1.99 +/- 0.19	0.025	
Fagus	2.35 +/- 0.11	0.057	
Fraxinus	1.03 +/- 0.11	0.022	
Quercus	5.83 +/- 0.15	0.035	
Salix	1.22 +/- 0.11	0.022	
Tilia	0.8 +/- 0.03	0.032	
Calluna vulgaris	0.82 +/- 0.02	0.038	Open land
Cerealia-t	1.85 +/- 0.38	0.06	
Cichorioideae	0.16 +/- 0.02	0.051	
Cyperaceae	0.87 +/- 0.06	0.035	
Ericaceae	0.07 +/- 0.04	0.038	
Gramineae	1 +/- 0	0.035	
Plantago lanceolata	1.04 +/- 0.09	0.029	
Plantago media	1.27 +/- 0.18	0.024	
Potentilla-t	1.19 +/- 0.13	0.018	

3.3 Evaluation of the LRA-based vegetation reconstruction

3.3.1 Testing strategy

This study uses pollen records from eight sites for the LRA-based vegetation reconstruction in the regional- and local/landscape-scales. Three categories of land-cover types are considered for evaluation: areas covered by conifers, broadleaved trees, and open land characterized by Ericaceous shrubs, graminoids and other herbaceous plants. The results - both the REVEALS-based estimates of regional vegetation and the LRA-based estimates of local vegetation - are evaluated against the

composition of those three categories of land cover regionally and locally. Both the GPM and LSM options are applied in the LRA as the pollen dispersal functions (as in section 2). Figure 4 summarizes the testing scheme described in this section, and Table 3 the nomenclature for the models, data sets used, and model outcomes.

Since pollen data are available only from small-sized sites < 4 ha (Table 1), we use a leave-one out strategy (LOO; Efron and Tibshirani, 1998; Sugita et al., 2010; Mazier et al., 2015) to avoid circularity in the LRA process: that is, selection of one site for local vegetation reconstruction with LOVE and the other seven sites for regional vegetation reconstruction with REVEALS. This process is repeated for all the eight sites in the study area. Theoretically and empirically the REVEALS results prove to be robust even when pollen data from several small-sized lakes and bogs are used (Sugita, 2007a; Sugita et al., 2010; Fyfe et al., 2013; Trondman et al., 2016; Hjelle et al. 2018; and others), although error estimates would be large. Hereafter, the REVEALS-based estimates of regional vegetation is referred to as RVs_LOO.

Another set of estimates for the regional vegetation composition within a 50-km radius from individual sites is compiled from the land-cover maps (section 3.2) and used as inputs for the LOVE application, independently and separately from RVs_LOO; hereafter, the data set is referred to as RVs_MAP50. Both RVs_LOO and RVs_MAP50 are then applied for reconstruction of the local/landscape-scale vegetation composition within the relevant source area of pollen (RSAP) with

339 the LOVE model for comparison. The inverse modeling of LOVE (Sugita, 2007b; Sugita et al., 2010)
340 is applied for estimating the RSAP with RVs_MAP50 around the plateaus of Bassiès in the three time
341 windows.

342 In addition, RVs_MAP50 is compared to the REVEALS results using pollen records from all
343 the eight sites together, referred to as RVs, to evaluate the extent to which the pollen-based
344 reconstruction reflects the observed vegetation composition of the region for the sake of simplicity.
345 The differences between RVs and individual RVs_LOO are negligible.

346 The LOVE results with either RVs_LOO or RVs_Map50 are evaluated against the plant
347 composition data extracted from the observed local land-cover maps in each time window. The
348 proportions of the areas (m^2) occupied by each land-cover type are estimated in successive concentric
349 rings at 20-m increment out to 2 km from the center of each site. Cumulative estimates of plant
350 composition within a 2-km radius are calculated, using a distance weighting method (either with the
351 LSM or GPM option) and fall speed of pollen for the 20 taxa as listed in Table 2. For all the
352 calculations this study uses ArcGIS 10.2.2, a script in R (Binet, unpublished) and
353 "DWPAcalculator.v7.3a" (Sugita, unpublished).

354

355

356

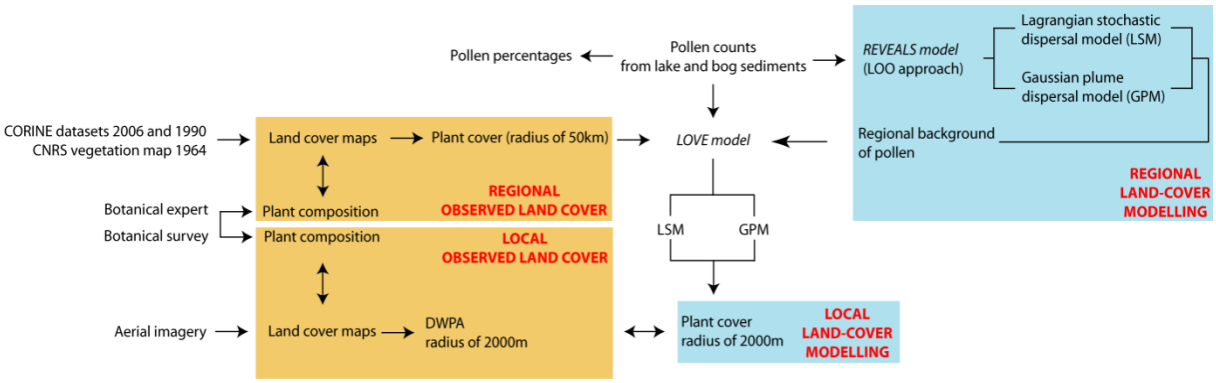

Figure 4 Flow chart of the methodological approach. LOO: Leave One Out approach. DWPA: Distance weighted plant abundance.

Table 3 Nomenclature

Model data/name	Meaning
LRA	Landscape Reconstruction Algorithm: REVEALS + LOVE models
REVEALS	Model for regional land-cover reconstruction
LOVE	Model for local land-cover reconstruction
POLLSCAPE	Model for landscape simulation
DWPA	Distance Weighted Plant Abundance
RSAP	Relevant Source Area of Pollen
RPP	Relative Pollen Productivity estimates
GPM	Gaussian Plume Model as pollen dispersal model
LSM	Lagrangian Stochastic Model as pollen dispersal model
RVs	The eight pollen archives are used with REVEALS
RVs-LOO	Seven pollen archives are used with REVEALS; LOO: Leave One Out approach
RVs-MAP50	Regional land-cover reconstruction based on the CORINE map
SE	Standard errors
LRA-LOO	Local vegetation estimates for a RSAP of 2-km radius with RVs-LOO as regional background of pollen
LRA-MAP50	Local vegetation estimates for a RSAP of 2-km radius with RVs-MAP50 as regional background of pollen

367 *3.3.2 Assumptions and parameter setting for the LRA calculation*

368 We use the pollen count data from three lakes and five bogs as inputs to the LRA. Our
369 preliminary trials (not shown) show that the selection of basin type (i.e. lake or bog) does not affect
370 the outcomes significantly; accordingly all the REVEALS and LOVE applications assume that the
371 pollen data used are from bogs. For model calculations this study uses a set of RPPs and fall speed of
372 pollen from Mazier et al. (2012) (Table 2) that is used in the LANDCLIM project (Trondman et al.,
373 2015; Marquer et al., 2014, 2017) and other projects in Europe.

374 A previous study (Mazier et al., 2015) shows that rare taxa can influence the LRA and RSAP
375 estimates. We therefore apply a threshold of 1 % to select the major pollen taxa recorded in both the
376 pollen and observed vegetation data sets. Accordingly, eighteen taxa are selected. Two additional
377 taxa (fir and juniper), locally important for the vegetation history of the Vicdessos valley, are added;
378 twenty taxa in total (Table 2). These plant/pollen types include both anemophilous and entomophilous
379 taxa.

380 We use "LRA.REVEALS.v6.2.2.exe" and "LRA.LOVE.v6.2.3.exe" for data analysis (Sugita,
381 unpublished). When the GPM option is used, pollen dispersal in a neutral atmospheric condition is
382 assumed with wind speed of 3 $msec^{-1}$ (although the local wind speed varies mostly between 0 and 4
383 $msec^{-1}$ (Szczypta et al., 2015; Claustres, 2016)). Z_{max}, the maximum spatial extent of the regional
384 vegetation from the centre of the study sites, is set to 50 km as in Mazier et al. (2012, 2015). When

385 the LSM option is applied, Z_{max} is automatically set to 100 km; all other conditions and parameters
386 specific to the model are the same as those in Kuparinen et al. (2007) and Theuerkauf et al. (2016).
387 The REVEALS and LOVE results are expressed in proportion cover for three land-cover
388 types: conifers, broadleaved trees, and open-land taxa (Table 2); their standard errors are obtained
389 according to the delta method (Stuart and Ord, 1994).
390 The regional plant composition based on the CORINE maps – RVs_MAP50 – do not have
391 error estimates (SEs), and these estimates are needed as inputs for the LOVE runs. We therefore have
392 calculated SEs for RVs_MAP50 by taking into account both SEs that were previously obtained from
393 RVs and both GPM and LSM options as follow:

394 $$SE_i = \frac{\frac{SE_{RV_{GPM}}i}{RV_{GPM}i} + \frac{SE_{RV_{LSM}}i}{RV_{LSM}i}}{2} \times RV_{MAP50}i$$

395 where $SE_{RV_{GPM}}i$ and $SE_{RV_{LSM}}i$ are the standard errors for species i of RVs using the GPM ($RV_{GPM}i$
396) and LSM ($RV_{LSM}i$) option, respectively. $RV_{MAP50}i$ is RVs_MAP50 for the species i.
397
398 **4. RESULTS**
399 **4.1 Estimates of the regional vegetation composition**
400 When the forested (i.e. conifers and broadleaved trees together) and unforested (i.e. open land)
401 covers are concerned, the REVEALS results (RVs) are largely overestimating open land, in particular

402 the ones using the LSM, in comparison to the observed data (RVs_MAP50); on the other hand,
403 forested areas are overestimated by pollen proportions alone (the left graph in Figure 5). In general,
404 RVs (with pollen data from all sites) using REVEALS with either the GPM or the LSM are more
405 dissimilar to the CORINE-map based estimates (RVs_MAP50) than pollen proportions alone.

406 The right graph of Figure 5 depicts the results along three axes of land cover types: open land,
407 conifers and broadleaved trees. Conifers and broadleaved trees are overestimated in pollen
408 proportions in comparison to RVs_MAP 50. Open land cover is overestimated in RVs relative to
409 RVs_MAP50. RVs with the GPM tend to be more similar to RVs_MAP50 than RVs with the LSM.

410

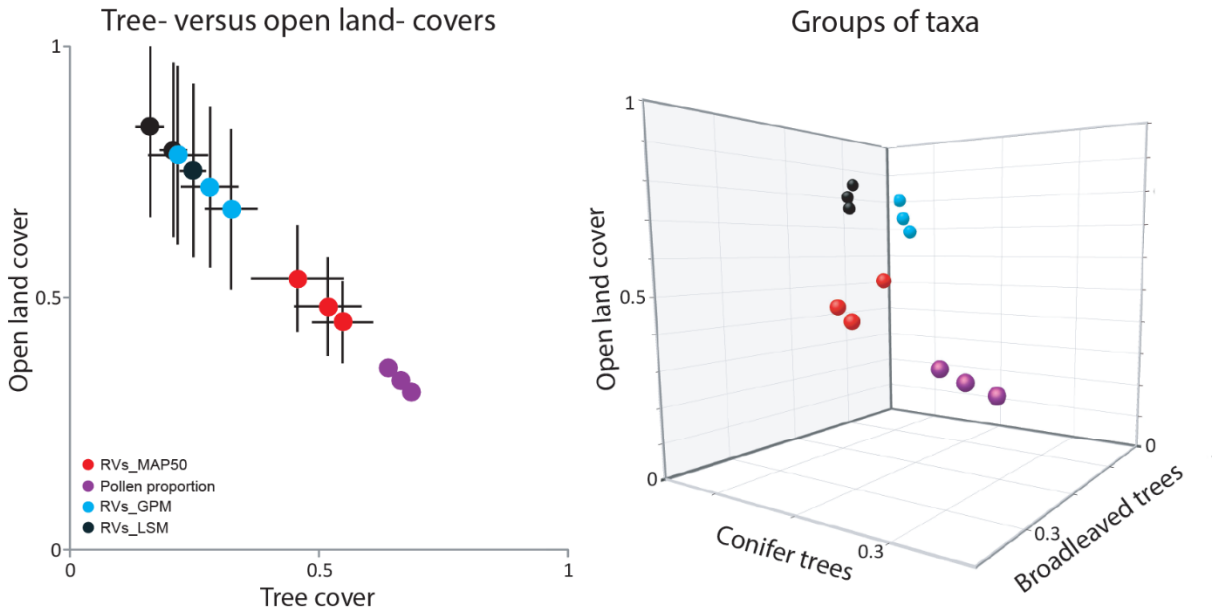

411

412 **Figure 5** Differences between RVs_MAP50 (i.e. observed regional land-covers for 2006, 1990 and 1964), pollen
413 proportions (untransformed pollen data) and REVEALS (RVs) using all local pollen records together for the three time
414 windows, 2013-2000, 2000-1990 and 1970-1960. REVEALS estimates have been calculated using both pollen dispersal
415 model alternatives, GPM and LSM. Results are shown for tree- versus open land- cover and groups of taxa (conifer trees,
416 broadleaved trees and open land taxa). The error bars are shown for the tree-versus open land-covers.

417 Standard errors of RVs for the open land category are larger than those for the forested areas
418 in general. Standard errors for pollen proportions, which represent the counting errors of pollen grains
419 are too low to be plot in Figure 5.
420
421 **4.2 Relevant source area of pollen (RSAP)**
422 The RSAP estimates for the three time windows vary from 663 to 1038 m with the GPM
423 option and from 1933 to 5113 m with the LSM option (Table 4); the former is consistently lower than
424 the latter in each time window. In four cases out of six, the RSAP estimates is lower than 2 km; the
425 two extreme values >4.5 km occur in the time windows of 1960-1970 and 2000-2013 with the LSM
426 option. Hereafter we assume that the area within a 2-km radius from each site is appropriate as the
427 RSAP and the reasonable spatial scale for the local/landscape scale reconstruction of vegetation in
428 the area. Possible reasons for the two extreme estimates of the RSAP will be considered in the
429 discussion section.
430
431 **Table 4** The relevant source areas of pollen (RSAP) based on LOVE runs using RVs_MAP50 as regional vegetation
432 background in LOVE. For all RSAP calculations both pollen dispersal model options have been tested, GPM and LSM.
433

	RVs_MAP50_2006	**RVs_MAP50_1990**	**RVs_MAP50_1964**
RSAP - GPM	1038 m	888 m	663 m
RSAP - LSM	4693 m	1933 m	5113 m

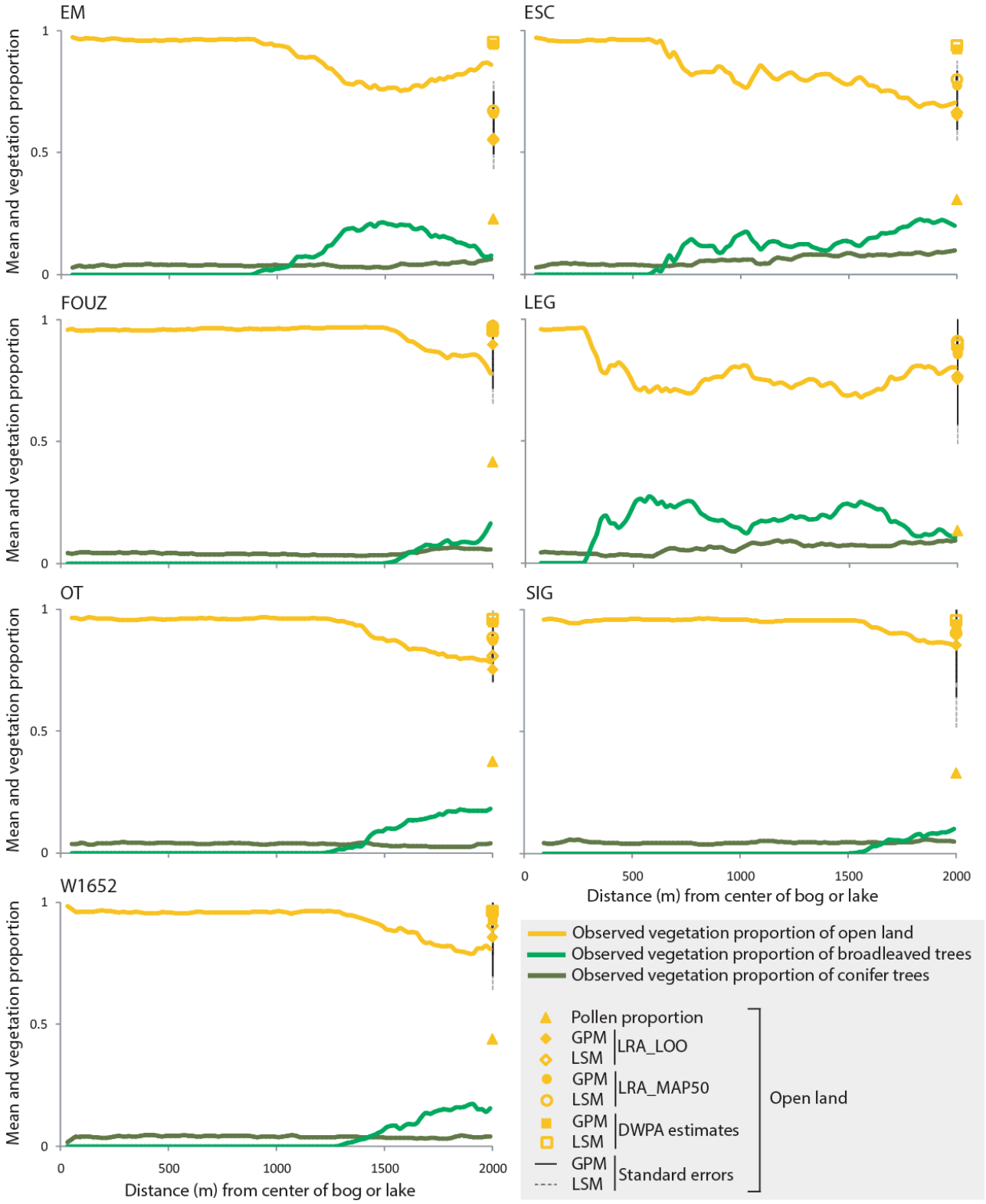

Figure 6 Spatial distribution of observed vegetation proportion based on local maps at a scale of incremental 20-m rings from the center of each site. Results are shown for the three groups of taxa, i.e. open land, broadleaved and conifer trees. Mean pollen proportion (untransformed pollen data) and LRA and DWPA estimates are given at a distance 2 km for each site. Note that pollen proportion, LRA and DWPA estimates are means over the whole 2 km. Results from all alternative scenarios we have used in this study are shown as well as the standard errors, for open land category. All data presented in this figure correspond to the time window 2013-2000. See Table 1 and Figure 2 for labels and site locations.

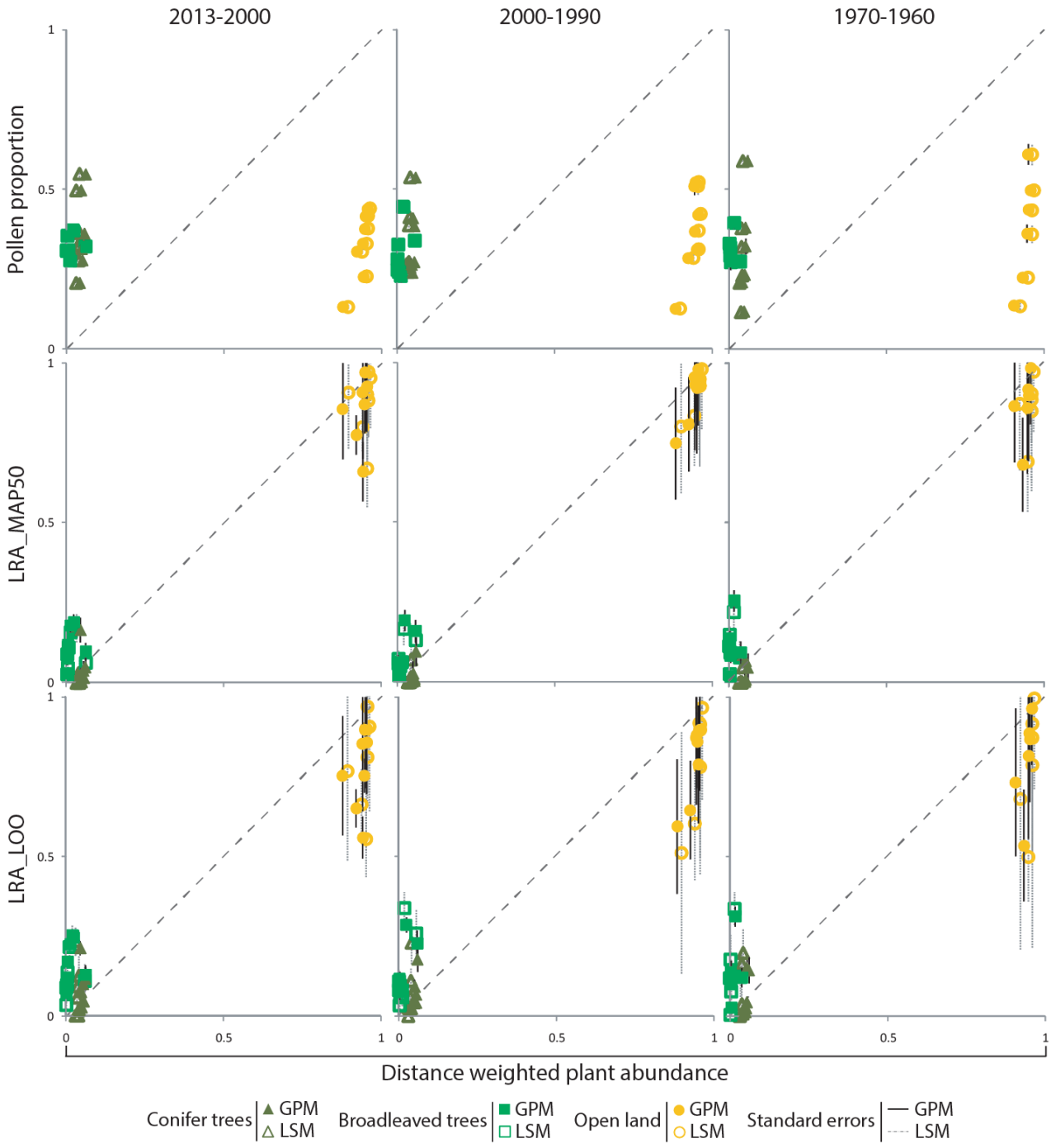

Figure 7 Comparison distance weighted plant abundance based on observed local land-cover maps against pollen proportion (untransformed pollen data) and two sets of LRA estimates, LRA_MAP50 and LRA-LOO (see text for further explanation). The results are shown for the three studied time windows. Each point represents a site. Pollen proportions and LRA estimates are reasonable representation of observed local land-cover (expressed here as distance weighted plant abundance) when pollen records are close to the dashed line.

450 **4.3 Evaluation of the LRA-based reconstruction of vegetation within a 2-km radius**

451 *4.3.1 Relationship between the spatial structure of plant composition and the LRA results*

452 Figure 6 summarizes the spatial distribution of the three land-cover types in proportion from
453 the basin shore out to 2 km at each site in the 2000-2013 window. Additional information is plotted
454 at the right end of each graph at each site, including (1) pollen proportion of plant types that indicate
455 open land, (2) the LRA-based estimates of open-land cover within a 2-km radius, with various
456 calculation settings tested (in a distance-weighted fashion; Sugita, 2007b), and (3) the cumulated
457 DWPA at 2 km from the center of each site (expressed in proportion) calculated from the local land-
458 cover maps. The LOVE model reconstructs the local vegetation in proportion based on the cumulative
459 DWPA within the RSAP (Sugita, 2007b) as a whole; thus, it is theoretically hard to look into the
460 spatial structure of local vegetation within the RSAP in detail. Figure 6 assists to visualize better the
461 extent to which the spatial structure of the local land cover would influence the LRA results in the
462 study area. Note that ARBU belongs to another watershed and detailed maps of the local land cover
463 are unavailable; therefore we do not include the site information in the figure.

464 Open land characterizes the immediately surrounding areas around individual sites. The
465 distances, at and beyond which tree covers (mostly broadleaved trees) increase, vary site to site: 270,
466 650, 900, 1250, 1300, 1500 and 1600 m at LEG, ESC, EM, OT, W1652, FOUZ and SIG, respectively.
467 The broadleaved-tree cover rises up to 10, 16, 17, 18, 21, 22 and 25% within a 2-km radius at SIG,

468 FOUZ, W1652, OT, EM, ESC and LEG, respectively.

469 Except for the EM site, the LRA-based reconstruction of open land is mostly in good
470 agreement with the estimates based on the cumulated DWPAs at 2 km from each site. LRA_LOO for
471 open land varies between 65 and 97% and LRA_MAP50 between 77.5 and 97% among the sites,
472 whereas the open-land proportion based on the cumulative DWPA ranges from 88 to 96%; all those
473 results consider the vegetation cover within a 2-km radius as a whole. At those seven sites the open-
474 land cover from the shore out to 2 km changes from 68 to 98.5%. The EM site is an exception. The
475 LRA-based results of open land at EM are underestimated, relative to the estimate based on the
476 cumulative DWPA; both LRA_LOO and LRA_MAP50 vary between 55 and 67%, but the cumulative
477 DWPA-based estimates range from 94 to 95%. The range of the changes in open land from the shore
478 out to 2 km is from 75 to 97% at EM.

479 The pollen proportions representing the open-land cover vary between 13 and 43% among the
480 sites, and thus significantly underestimate both the cumulative DWPA-based estimates and the
481 observed proportions of the open-land cover within a 2-km radius (Figure 6). Three graphs in the top
482 row of Figure 7 also demonstrate clearly that pollen proportions alone do not correspond to the
483 DWPA-based estimates of all the three land-cover types within a 2-km radius in all time windows.
484 Although expected, those results reaffirm that the LRA-based results are more realistic than pollen
485 proportions alone in reconstruction of vegetation and land cover in mountains such as our study area.

4.3.2 The LRA estimates and factors affecting their reliability in three time windows

Against the cumulative DWPA-based estimates of vegetation cover within a 2-km radius, LRA_MAP50 is a better choice for all the land-cover types than LRA_LOO in the three time windows (Figure 7). Relative to the LRA_LOO results (the bottom row of Figure 7), the LRA_MAP50 estimates tend to have smaller standard errors at individual sites, to have smaller site-to-site variations for each land-cover type, and to be closer to the 1:1 relationship against the cumulative DWPA-based estimates (the middle row of Figure 7). These patterns are apparent for the open-land cover estimates in particular. For example, the differences between the highest and lowest LRA_MAP50 estimates are 32, 23 and 30%, and 42, 46 and 49% when LRA_LOO is concerned, in time windows 2013-2000, 2000-1990 and 1970-1960, respectively. The site-to-site variation of the LRA estimates does not change significantly among the three time-windows when LRA_MAP50 is considered; when LRA_LOO is concerned, however, the older the time window, the larger the site-to-site variation of the LRA estimates for each land-cover type.

This study shows that selection of a pollen dispersal model, either the GPM or the LSM option, does not affect significantly the LRA-based reconstruction of vegetation cover within the RSAP since the 1960s (Figure 7) as long as the model selection is consistent in the entire LRA process. However, the selection appears influencing the magnitude of uncertainties. With the LSM option, the SEs of

LRA_LOO for open land vary from 10.5-57 %; on the other hand, those vary from 5.2 to 26.1% with the GPM option. When LRA_MAP50 is concerned, the differences influenced by the selection of the dispersal model are negligible: the SEs vary from 7.4 to 25.2% with the LSM option and from 5.2 to 26.1 % with the GPM option. As suggested in the simulations in section 2**,** the systematic selection of pollen sites in mountains, which is the case for RVs_LOO (and thus affecting LRA_LOO), is a suspect for those results on the differences in the SEs.

5. DISCUSSION

Pollen proportions are notoriously difficult to use for reconstruction of mountain vegetation (Markgraf, 1980; Fall, 1992; Birks and Birks, 2000; Ortu et al., 2006; Leunda et al., 2017). This study demonstrates that the LRA approach improves reconstruction of vegetation and land cover in mountains greatly over pollen percentages alone. The assumptions and conditions for the LRA are too simple for landscapes with complex topography and wind field in mountain regions. However, the simulations (section 2) and the application results in the Vicdessos area show that some of the difficult issues associated with pollen-based reconstruction of vegetation in mountains can be addressed and overcome.

522 *5.1. Effects on the LRA results of systematic selection of pollen sites on mountain*

523 Pollen-based reconstruction of mountain vegetation often selects small-sized pollen sites only
524 in mountains and high-altitude plateaus. This site-selection strategy is useful for evaluating site-
525 specific correlational relationships between pollen assemblages and the surround vegetation; however,
526 it makes the LRA-based quantitative reconstruction of vegetation difficult. The REVEALS-based
527 estimates of regional vegetation – an important outcome from the first step of the LRA- are critical
528 for evaluating the abundance of long-distance pollen from the regional sources that are assumed to
529 be consistent among small-sized sites for the LOVE applications. However, when several small-sized
530 sites are selected above the tree line on the same land cover type, we expect biased estimates of the
531 regional vegetation within a 50-100 km radius. This is the case in our study in the Vicdessos area
532 (Figure 5); the regional components of the open land cover are overestimated by REVEALS. Because
533 pollen records from small-sized sites tend to represent local vegetation (Prentice, 1985; Sugita, 1994),
534 we expect that the REVEALS results based on pollen records from those sites underestimate the
535 abundances of tree covers in the region.

536 One of the solutions to reduce the biases described above is to use large lakes (known as
537 regional reliable pollen archives; Sugita, 2007a; Trondman et al., 2016) and/or several small sites
538 (lakes and bogs) located in various valleys, slopes and altitudes in the region, although reliable pollen
539 sites in mountains are mainly small and located in sub-alpine or alpine zones (Simonneau et al., 2013).

Abraham et al. (2017) used pollen records from small sites located above and below the treeline in low mountain ranges of NE Czech Republic and obtained reasonable REVEALS estimates of past regional vegetation. Hjelle et al. (2015) have used pollen samples from one large lake and twenty-eight small lakes located in different types of vegetation in western Norway. They found a good relationship between the REVEALS estimates and CORINE land-cover data, although the REVEALS model tends to overestimate open land cover against the CORINE land-cover. Hjelle et al. further show that the higher the number of small lakes, the more reliable the REVEALS estimates. Thus, establishing a proper site-selection scheme is the important step for REVEALS applications, although it is hard to find a large number of suitable pollen sites in mountain regions.

As expected, the LRA results using RVs_MAP50 are better matched with the map-based DWPAs within a 2-km radius than those using RVs_LOO (Figure 7). Standard errors of LRA_MAP50s are smaller than those of LRA_LOOs, in general. Those results demonstrate the importance of the accuracy and reliability of the regional estimates of vegetation and land cover for the LRA approach. Even so, it's also encouraging that the RVs_LOOs are usable to provide robust estimates of LRA_LOOs using our data set.

558 *5.2 Selection of pollen dispersal models for mountain situations*

559 The differences in the LRA results with the LSM and GPM options are negligible in the
560 simulations and the empirical study at the Vicdessos area (Figure 7). A LSM scheme is more
561 advanced and realistic in description of atmospheric airflow and long-distance particle dispersal than
562 a GPM scheme (Kuparinen et al., 2007). Comparisons between REVEALS_LSM and
563 REVEALS_GPM (Theuerkauf et al., 2013, 2016) using pollen records from lakes in NE Germany
564 showed the superiority of the use of the LSM of Kuparinen et al. (2007) over the GPM traditionally
565 used in pollen-based vegetation modelling. Mariani et al. (2017) came to the same conclusion based
566 on their study in Tasmania. We expected that applications of the LSM would improve the LRA results,
567 in particular reducing biases on the long-distance pollen from the regional source, caused by complex
568 topography and wind field in mountains. However, our results show that the REVEALS_GPM-based
569 estimates of the regional vegetation cover tend to be closer to the observed regional land-cover than
570 those by REVEALS_LSM (Figure 5); the LSM and GPM options do not influence significantly the
571 LOVE results.

572 The LSM takes into account higher updraft velocities in air via turbulence better than the
573 GPM (Kuparinen et al., 2007); thus, heavier pollen types, such as *Abies* and *Fagus*, tend to be
574 modeled to disperse further with the LSM than with the GPM (Sutton, 1953). The consequence is
575 that GPM gives greater importance to pollen arriving from shorter distances, especially for pollen

types with high fall speed of pollen, than the LSM does (Kuparinen et al., 2007; Theuerkauf et al., 2013), and in our study this is the cause of the underestimation of *Abies* and *Fagus* based on LSM, and thereby of the overestimation of regional open land based on LSM.

Size of pollen-sampling sites may be one of the possible reasons why the LRA estimates with the LSM option do not improve significantly against those with the GPM option. Indeed, the LSM would be a better option for pollen dispersion and deposition in large lakes than the GPM; pollen dispersion and deposition in such lakes are greatly affected by turbulent flows and updrafts (Jackson and Lyford, 1999), thus the LSM is more appropriate than the GPM. However, short-distance dispersal of pollen is better described by the GPM than by the LSM (Theuerkauf et al., 2016); accordingly, the GPM option would be better suited for reconstruction of vegetation using pollen records from small bogs and lakes like in the Vicdessos, where asymmetric airflows would play a minor role locally. As a consequence, selection of a pollen dispersal model would affect the LRA results little, when small sites are used. Standard errors are higher using LSM than using GPM, however, as the simulations (section 2) demonstrate.

Another important issue is the availability of the estimates of relative pollen productivity, RPP, for the constituent taxa used for data analysis. This study uses RPPs that were compiled from previous studies in NW Europe; those studies used the Extended R-value models to obtain RPPs, assuming that pollen dispersal follows the GPM (e.g. Sugita, 1994; Broström et al., 2008; Mazier et al., 2012).

Ideally, when the LSM is used for the LRA, RPPs need to be obtained from other data sets by assuming the LSM as a pollen dispersal model for consistency. Theuerkauf et al. (2013, 2016) obtained RPPs of selected taxa in lowlands in North Germany; however, Asteraceae and Ericaceae, important taxa in our study, are not included. Mariani et al. (2016, 2017) estimated RPPs for selected taxa in Tasmania. Thus far, the LSM-based estimates of RPPs are available from one study only in NE Germany; considering their variations caused by various environmental and anthropogenic factors, it is necessary to expand the database of the LSM-based RPPs for further applications of the LSM in the LRA reconstruction. All things considered, it is justified for this study to use RPPs for the selected taxa from NW Europe (Mazier et al., 2012; Trondman et al., 2015; Marquer et al., 2014, 2017).

5.3 The LRA-based reconstruction of vegetation composition with insect-pollinated plants

Plant communities at the mountain tops in our study region are characterized by high abundance of insect-pollinated taxa such as Ericaceae (e.g. *Rhododendron* spp. and *Vaccinium* spp.) with semi-dominant grass and *Calluna* (heather). Ericaceae plants have low pollen production (see Table 2) relative to the wind-pollinated taxa in general (Mazier et al., 2012); then fall speed of pollen being similar among the constituent taxa, the LRA estimates of Ericaceae, thus the open land cover, tend to increase relative to the other taxa and land cover types. Mazier et al. (2012) excluded

612 zoophilous taxa from the REVEALS reconstruction, mainly because the model assumes that all pollen
613 grains are coming via wind transport. However, the majority of the upland plant taxa common on
614 mountain tops are zoophilous. It is ecologically important to include zoophilous taxa in pollen-based
615 reconstruction of vegetation. Mariani et al. (2017) used both wind- and animal-pollinating plant taxa
616 together for the REVEALS applications in Tasmania successfully. In the Pyrenees, this study also
617 demonstrates that the LRA approach appears working reasonably well with zoophilous taxa for
618 reconstruction of the vegetation and land cover in the local- and landscape-scales. This suggests that
619 entomophilous taxa that are preserved in sediments might also be transported by wind.
620
621 *5.4 Relevant source area of pollen (RSAP) and LRA estimates of local vegetation in mountains*
622 In theory and practice the RSAP is the smallest spatial scale possible for pollen-based
623 reconstruction of vegetation (Sugita, 1994, 2007b, 2013; Sugita et al., 2010). In the current LRA form
624 (Sugita, 2007a, 2007b), the LRA result is expressed in proportions of the total cumulative sum of
625 plant abundance at the RSAP (e.g., in biomass, plant cover, foliage mass, basal area, etc.) that is
626 measured in a distance-weighted fashion for all the constituent taxa. Interpretation of the LRA results
627 can be confusing, however. A cumulative sum of the DWPA is a way how pollen records reflect the
628 surrounding vegetation (Prentice, 1984, 1988; Sugita, 1994; Sugita et al., 2010), and the LRA results
629 are based on the cumulative DWPA at the RSAP (Sugita, 2007b). According to this view on the

630 pollen-vegetation relationship, the site-specific spatial structure of vegetation within the RSAP is
631 impossible to assess quantitatively. Figure 6 is an attempt to visualize how different the spatial
632 structure of the surrounding vegetation at individual sites could be, even when the LRA results are
633 relatively similar among most of the sites.

634 The RSAP estimates (Table 3), which are obtained with an inverse modeling of LOVE (Sugita,
635 2007b; Sugita et al., 2010), are significantly smaller with the GPM option than those with the LSM
636 option at all time windows. This is contradictory to the simulation results in section 2; the LRA-based
637 estimate of the RSAP with the GPM option (i.e. 310 m) is only slightly smaller than that with the
638 LSM option (i.e. 325 m). The GPM describes pollen dispersal in such a way that pollen grains,
639 especially heavy pollen types such as Ericaceae fall to the ground in shorter distances than the LSM
640 does (Kuparinen et al., 2007; Theuerkauf et al., 2016; see also section 5.2). On the other hand, the
641 LSM predicts higher abundance of long-distance pollen from the regional source, including arboreal
642 plants growing abundantly in lower altitudes, into mountain sites than the GPM does. All these factors,
643 as well as others (e.g., the spatial structure of mountain vegetation, non-random selection of pollen-
644 site location, and the lack of RPP estimates considering LSM) would interact and affect the LRA-
645 based estimates of the RSAP in unknown ways. Further studies are necessary.

646 Among the six RSAP estimates listed in Table 3, four estimates are close to or smaller than 2
647 km. The other two, which are obtained with the LSM option, are >4.5 km. Most of the previous

studies also show that the RSAP estimates are smaller than 2.8 km in radius, when pollen sites are small- to medium-sized (Sugita et al., 2010; Overballe-Petersen et al., 2013; Cui et al., 2013, 2014; Poska et al., 2014; Hjelle et al., 2015; Mazier et al., 2015; Abraham et al., 2017). In practice, the local vegetation maps are available only within a 2-km radius around each site for comparison, as well. All things considered, the area within a 2-km radius is appropriate to be used as the RSAP for the study, with which all the results in Figures 6 and 7 are obtained.

Figure 6 shows that the areas close to the sampling sites are mostly unforested; tree cover (mostly broadleaved trees) increases at and beyond 270-1600 m depending on the sites. The DWPA results depict that, with either the GPM or LSM option, the open-land cover is dominant consistently. Except for the EM site, the LRA_LOOs and LRA_MAP50s within a 2-km radius are reasonable against the DWPAs; these results assure the relevance of the LRA approach in this area. At the same time it is clear that the spatial structure of vegetation within the RSAP varies among sites significantly, even though the site-to-site variation of the LRA results is small. It's hard to speculate the site-specific spatial structure of vegetation within the RSAP based on the LRA approach or something else.

When the GPM option is selected, the radii of the LRA-based RSAP vary from 663 m (1960-1970) to 888 m (1990-2000) to 1038 m (2000-2013), indicative of a shift in the "grain size" of the spatial structure of the surrounding vegetation around the sites (Sugita, 1994; Bunting et al., 2004). It is reasonable to assume that changes in climate regimes and anthropogenic forcing in the area have

666 affected the spatial structure of vegetation and land cover constantly.

667

668 **6. CONCLUSIONS**

669 The main conclusions from this study are:

670 • The LRA approach is a significant improvement in pollen-based reconstruction of mountain
671 vegetation in the local- and landscape-scales over pollen percentages alone.

672 • Both the simulations and empirical model-data comparison in the Pyrenees demonstrate that
673 accuracy of the regional estimates of vegetation matters for reconstruction of the
674 local/landscape scale reconstruction of mountain vegetation in the LOVE applications.

675 • The REVEALS-based estimate of regional vegetation – the first step of the LRA – is
676 influenced by selection of pollen dispersal model and the systematic selection of pollen sites
677 on mountains. Historical land-cover maps are effective as an alternative source for the
678 regional vegetation in the last couple of centuries.

679 • Area within a 2-km radius appears to be a relevant spatial scale for the LRA reconstructions
680 in the Vicdessos area in the Pyrenees in the three time windows evaluated.

681 • Insect-pollinated plant taxa, often important to characterize vegetation in higher altitudes, can
682 be included and informative for the LRA-based vegetation reconstruction in mountains.

- Further clarification is necessary to better understand the pros and cons of two dispersal models – the Lagrangian Stochastic Model and Gaussian Plume model – for the LRA applications in mountain environments.

The present work provides an important basis for reliable palaeoecological reconstruction in the Pyrenees and for advances in research about the past and recent intense human impact in the region. Further studies will help improve some of the modelling approaches for a better understanding of the spatial and temporal distribution of plant taxa within a catchment (Plancher et al., in prep.) and the reconstruction of local paleorainfall by using the erosion processes (Allen et al., in press).

ACKNOWLEGEMEMNTS

This work is part of the TRAM (Trace metal legacy on mountains aquatic ecogeochemistry) and MODE-RESPYR (Modeling Past and future land cover changes in the Pyrenees) projects (supported by The French National Research Agency) coordinated respectively by G. Le Roux and T. Houet, the PEPS CNRS POPEYE « Du POllen aux PalEopaYsagEs montagnard, vers un développement méthodologique » project coordinated by F. Mazier and the Observatoire Hommes-Milieux Pyrénées Haut Vicdessos (Labex DRIIHM) research program coordinated by D. Galop. It is also a contribution to the PAGES LandCover6k working group (http://www.pastglobalchanges.org/ini/wg/landcover6k/intro) coordinated by M.J. Gaillard. S. Sugita

701 was partially supported by a grant from the Estonia Research Council (IUT18-09: the ENCHANTED
702 project). We thank ARTEMIS facility (CNRS-Gif sur Yvette, France) for radiocarbon dating of the
703 samples, and P. van Beek and M. Souhaut at the LAFARA underground laboratory where the
704 sediment samples have been analyzed for ^{210}Pb and ^{137}Cs to establish chronologies.

705

706 **REFERENCES**

707 Abrahama, V., Novák, J., Houfková, P. et al. (2017) A Landscape Reconstruction Algorithm and
708 pedoanthracological data reveal Late Holocene woodland history in the lowlands of the NE Czech
709 Republic. Review of Palaeobotany and Palynology, 244, 54-64.

710 Appleby, P.G. (2002) Chronostratigraphic Techniques in Recent Sediments. In: Last, W.M. & Smol,
711 J.P. (Eds.) Tracking Environmental Change Using Lake Sediments; Developments in
712 Paleoenvironmental Research. Springer Netherlands, pp. 171-203.

713 Allen, D. Simonneau, A., Le Roux, G. et al. (accepted for publication) Considering lacustrine erosion
714 records and the De Ploey erosion model in an examination of mountain catchment erosion
715 susceptibility and total rainfall reconstruction. Catena.

716 Binford, M.W. (1990) Calculation and uncertainty analysis of 210Pb dates for PIRLA project lake
717 sediment cores. Journal of Paleolimnology, 3, 253-267.

718 Birks, H.H. & Birks, H.J.B. (2000) Future uses of pollen analysis must include plant macrofossils.

719 Journal of Biogeography, 27, 31-35.

720 Blaauw, M. (2010) Methods and code for 'classical' age-modelling of radiocarbon sequences.

721 Quaternary Geochronology, 5, 512-518.

722 Broström, A., Sugita, S. & Gaillard, M.J. (2004) Pollen productivity estimates for the reconstruction

723 of past vegetation cover in the cultural landscape of southern Sweden. The Holocene, 14, 368-381.

724 Broström, A., Sugita, S., Gaillard, M.J. et al. (2005) Estimating spatial scale of pollen dispersal in the

725 cultural landscape of southern Sweden. The Holocene, 15, 252-262.

726 Bunting, M.J., Gaillard, M.J., Sugita, S. et al. (2004) Vegetation structure and pollen source area. The

727 Holocene, 14, 651-660.

728 Claustres, A. (2016) Répartition des éléments traces potentiellement toxiques dans les zones de

729 montagne : Rôle et part des facteurs naturels et anthropiques à l'échelle des temps pédologiques.

730 Thèse de doctorat de l'Université de Toulouse III Paul Sabatier.

731 Cui, Q.Y., Gaillard, M.J., Lemdahl, G. et al. (2013) The role of tree composition in Holocene fire

732 history of the hemiboreal and southern boreal zones of southern Sweden, as revealed by the

733 application of the Landscape Reconstruction Algorithm: implications for biodiversity and climate-

734 change issues. The Holocene, 23, 1747-1763.

735 Cui, Q.Y., Gaillard, M.J., Lemdahl, G. et al. (2014) Historical land-use and landscape change in

736 southern Sweden and implications for present and future biodiversity. Ecology and Evolution, 4,

737 3555-3570.

738 David, F. (1993) Altitudinal variation in the response of the vegetation to Late-glacial climatic events

739 in the northern French Alps. New Phytologist, 125, 203-220.

740 David, F. (1997) Holocene tree limit history in the northern French Alps stomata and pollen evidence.

741 Review of Paleobotany and Palynology, 97, 227-237.

742 MacDonald, D., Crabtree, J.R., Wiesinger, G. et al. (2000) Agricultural abandonment in mountain

743 areas of Europe: Environmental consequences and policy response. Journal of Environmental

744 Management, 59, 47-69.

745 Efron, B. & Tibshirani, R.J. (1998) An Introduction to the Bootstrap. Chapman & Hall/CRC, Boca

746 Raton.

747 Fall, P.L. (1992) Spatial patterns of atmospheric pollen dispersal in the Colorado Rocky Mountains,

748 USA. Review of Palaeobotany and Palynology, 74, 293-313.

749 Fyfe, R.M., Twiddle, C., Sugita, S. et al. (2013) The Holocene vegetation cover of Britain and Ireland:

750 overcoming problems of scale and discerning patterns of openness. Quaternary Science Reviews,

751 73, 132-148.

752 Gaillard, M.J., Sugita, S., Bunting, M.J. et al. (2008) The use of modelling and simulation approach

753 in reconstructing past landscapes from fossil pollen data: a review and results from the

754 POLLANDCAL network. Vegetation History and Archaeobotany, 17, 419-443.

755 Galop, D., Houet, T., Mazier, F. et al. (2011) Grazing activities and biodiversity history in the
756 Pyrenees: New insights on high altitude ecosystems in the framework of a Human-Environment
757 Observatory. Past Global Changes Magazine, 19, 53-55.
758 Galop, D., Rius, D., Cugny, C. et al. (2013) Long-term human-environment interactions history in
759 the French Pyrenean Mountains inferred from pollen data. In: Lozny, L. (ed.) Continuity and
760 Change in Cultural Adaptation to Mountain Environments. Studies in Human Ecology and
761 Adaptation 7. Springer Science + Business Media, New York, pp. 19-30.
762 Herrault, P.A., Larrieu, L., Cordier, S. et al. (2016) Combined effects of area, connectivity, history
763 and structural heterogeneity of woodlands on the species richness of hoverflies (Diptera:
764 Syrphidae). Landscape Ecology, 31, 877-893.
765 Hjelle, K.L. & Sugita, S. (2012) Estimating pollen productivity and relevant source area of pollen
766 using lake sediments in Norway: how does lake size variation affect the estimates? The Holocene,
767 22, 313-324.
768 Hjelle, K.L., Mehl, I.K., Sugita, S. et al. (2015) From pollen percentage to vegetation cover:
769 evaluation of the Landscape Reconstruction Algorithm in western Norway. Journal of Quaternary
770 Science, 30, 312-324.
771 Hjelle, K.L., Halvorsen, L.S., Prøsch-Danielsen, L. et al. (2018) Long-term changes in regional
772 vegetation cover along the west coast of southern Norway: The importance of human impact.

773 Journal of Vegetation Science, 29, 404-415.

774 Houet, T., Vacquié, L., Vidal, F. et al. (2012) Caractérisation de la fermeture des paysages dans les
775 Pyrénées depuis les années 1940. Application sur le Haut-Vicdessos. Sud-Ouest européen, 33, 41-
776 56.

777 Houet, T., Vacquié, L. & Sheeren, D. (2015) Evaluating the spatial uncertainty of future land
778 abandonment in a mountain valley (Vicdessos, Pyrenees-France): insights form model
779 parameterization and experiments. Journal of Mountain Science, 12, 1-18.

780 IPCC, 2014: Climate Change 2014: Synthesis Report. Contribution of Working Groups I, II and III
781 to the Fifth Assessment Report of the Intergovernmental Panel on Climate Change [Core Writing
782 Team, R.K. Pachauri and L.A. Meyer (eds.)]. IPCC, Geneva, Switzerland, 151 pp.

783 Jackson, S.T. & Lyford, M.E. (1999) Pollen dispersal models in Quaternary plant ecology:
784 assumptions, parameters, and prescriptions. The Botanical Review, 65, 39-75.

785 Kozak, J., Gimmi, U., Houet, T. & Bolliger, J. (2017) Current practices and challenges for modelling
786 past and future land use and land cover changes in mountainous regions. Regional Environmental
787 Change, 17, 2187-2191.

788 Kuparinen, A., Markkanen, T., Riikonen, H. et al. (2007) Modeling air-mediated dispersal of spores,
789 pollen and seeds in forested areas. Ecological Modelling, 208, 177-188.

790 Leunda, M., González-Sampériz, P., Gil-Romera, G. et al. (2017) The Late-Glacial and Holocene

791 Marboré Lake sequence (2612 m a.s.l., Central Pyrenees, Spain): Testing high altitude sites
792 sensitivity to millennial scale vegetation and climate variability. Global and Planetary Change,
793 157, 214-231.
794 Leunda, M., González-Sampériz, P., Gil-Romera, G. et al. (2019) Ice cave reveals environmental
795 forcing of long-term Pyrenean tree line dynamics. Journal of Ecology, 107, 814-828.
796 Mariani, M., Connor, S., Theuerkauf, M. et al. (2016) Testing quantitative pollen dispersal models in
797 animal-pollinated vegetation mosaics: An example from temperate Tasmania, Australia.
798 Quaternary Science Reviews, 154, 214-225.
799 Mariani, M., Kuneš, P. Connor, S.E. et al. (2017) How old is the Tasmanian cultural landscape? A
800 test of landscape openness using quantitative land-cover reconstructions. Journal of Biogeography,
801 44, 2410-2420.
802 Markgraf, V. (1980) Pollen Dispersal in a Mountain Area. Grana, 19, 127-146.
803 Marquer, L., Gaillard, M.J., Sugita, S. et al. (2014) Holocene changes in vegetation composition in
804 northern Europe: why quantitative pollen-based vegetation reconstructions matter. Quaternary
805 Science Reviews, 90, 199-216.
806 Marquer, L., Gaillard, M.J., Sugita, S. et al. (2017) Quantifying the effects of land-use and climate
807 on Holocene plant composition and vegetation change in Europe. Quaternary Science Reviews,
808 171, 20-37.

809 Mazier, F., Gaillard, M.J., Kuneš, P. et al. (2012) Testing the effect of site selection and parameter
810 setting on REVEALS-model estimates of plant abundance using the Czech Quaternary
811 Palynological Database. Review of Palaeobotany and Palynology, 187, 38-49.
812 Mazier, F., Broström, A., Bragée, P. et al. (2015) Two hundred years of land-use change in the South
813 Swedish Uplands: comparison of historical map-based estimates with a pollen-based
814 reconstruction using the landscape reconstruction algorithm. Vegetation History and
815 Archaeobotany, 24, 555-570.
816 Ortu, E., Brewer, S. & Peyron, O. (2006) Pollen-inferred palaeoclimate reconstructions in mountain
817 areas: problems and perspectives. Journal of Quaternary Science, 21, 615-627.
818 Overballe-Petersen, M.V., Nielsen, A.B. & Bradshaw, R.H.W. (2013) Quantitative vegetation
819 reconstruction from pollen analysis and historical inventory data around a Danish small forest
820 hollow. Journal of Vegetation Science, 24, 755-771.
821 Poska, A., Saarse, L., Koppel, K. et al. (2014) The Verijärv area, South Estonia over the last
822 millennium: a high resolution quantitative land cover reconstruction based on pollen and historical
823 data. Review of Palaeobotany and Palynology, 207, 5-17.
824 Prentice, I.C. (1985) Pollen representation, source area, and basin size: toward a unified theory of
825 pollen analysis. Quaternary Research, 23,76-86.
826 Prentice, I.C. (1988) Records of vegetation in time and space: the principles of pollen analysis. In:

827 Huntley, B. & Webb, T. (Eds.) Vegetation history. Kluwer, Dordrecht, pp. 17-42.

828 Quintana-Seguí, P., Le Moigne, P., Durand, Y. et al. (2008) Analysis of Near-Surface Atmospheric
829 Variables: Validation of the SAFRAN Analysis over France. Journal of Applied Meteorology and
830 Climatology, 47, 92-107.

831 Randall, P.M. (1990) A study of modern pollen deposition, Southern Alps, South Island, New
832 Zealand. Review of Palaeobotany and Palynology, 64, 263-272.

833 Simonneau, A., Chapron, E., Courp, T. et al. (2013) Recent climatic and anthropogenic imprints on
834 lacustrine systems in the Pyrenean Mountains inferred from minerogenic and organic clastic
835 supply (Vicdessos valley, Pyrenees, France). The Holocene, 23, 1762-1775.

836 Stuart, A. & Ord, J.K. (1994) Kendall's advanced theory of statistics. Volume 1. Distribution theory.
837 Edward Arnold.

838 Sugita, S. (1993) A model of pollen source area for an entire lake surface. Quaternary Research, 39,
839 239-244.

840 Sugita, S. (1994) Pollen representation of vegetation in Quaternary sediments: Theory and method in
841 patchy vegetation. Journal of Ecology, 82, 881-897.

842 Sugita, S. (2007a) Theory of quantitative reconstruction of vegetation I: Pollen from large sites
843 REVEALS regional vegetation composition. The Holocene, 17, 229-241.

844 Sugita, S. (2007b) Theory of quantitative reconstruction of vegetation II: All you need is LOVE. The

845 Holocene, 17, 243-257.

846 Sugita, S. (2013) Pollen methods and studies, POLLSCAPE Model: Simulation Approach for Pollen
847 Representation of Vegetation and Land Cover. In: Scott A. Elias (Ed) Encyclopedia of Quaternary
848 Science (Second Edition). Elsevier, Amsterdam, pp. 871-879.

849 Sugita, S., MacDonald, G.M. & Larsen, C.P.S. (1997) Reconstruction of fire disturbance and forest
850 succession from fossil pollen in lake sediments: potential and limitations. In: Clark, J.S., Cachier,
851 H. et al. (Eds.) Sediment Records of Biomass Burning and Global Change. Springer, Berlin, pp.
852 387-412.

853 Sugita, S., Gaillard, M.J. & Broström, A. (1999) Landscape openness and pollen records: a simulation
854 approach. The Holocene, 9, 409-421.

855 Sugita, S., Hicks, S. & Sormunen, H. (2010) Absolute pollen productivity and pollen-vegetation
856 relationships in northern Finland. Journal of Quaternary Science, 25, 724-736.

857 Sutton, O.G. (1953) Micrometeorology. McGraw-Hill.

858 Szczypta C., Gascoin S., Houet T., Vigneau C. & Fanise P. (2015) Impact of climate and land cover
859 changes on snow cover in a small Pyrenean catchment. Journal of Hydrology, 521, 84-99.

860 Theuerkauf, M., Kuparinen, A. & Joosten, H. (2013) Pollen productivity estimates strongly depend
861 on assumed pollen dispersal. The Holocene, 23, 14-24.

862 Theuerkauf, M., Couwenberg, J., Kuparinen, A. et al. (2016) A matter of dispersal: REVEALSinR

863 introduces state-of-the-art dispersal models to quantitative vegetation reconstruction. Vegetation
864 History and Archaeobotany, 25, 541-553.
865 Trondman, A.K., Gaillard, M.J., Mazier, F. et al. (2015) First pollen-based quantitative
866 reconstructions of Holocene regional vegetation cover (plant functional types and land-cover
867 types) in Europe suitable for climate modelling. Global Change Biology, 21, 676-697.
868 Trondman, A.K., Gaillard, M.J., Sugita, S. et al. (2016) Are pollen records from small sites
869 appropriate for REVEALS model-based quantitative reconstructions of past regional vegetation?
870 An empirical test in southern Sweden. Vegetation History and Archaeobotany, 25, 131-151.
871 Tutin, T.G., Heywood, V.H., Burgess, N.A. et al. (1964–1980) Flora Europaea. Cambridge
872 University Press: Cambridge, UK.
873 Vacquié, L., Houet, T., Sheeren, D. et al. (2016) Adapting grazing practices to limit the reforestation
874 of mountainous summer pastures: A process-based approach. Environmental Modelling &
875 Software, 84, 395-411.
876 Zhang, Y., Kong, Z., Yang, Z. et al. (2017) Surface Pollen Distribution from Alpine Vegetation in
877 Eastern Tibet, China. Scientific Reports, 7, 586: doi: 10.1038/s41598-017-00625-7.
878
879
880

881

882

883

884

885

886 **APPENDICES**

887 **Appendix A.** POLLSCAPE simulation and evaluation of the Landscape Reconstruction Algorithm

888 for mountain regions.

889 **Appendix B.** Dated materials and details on age-depth models of sedimentary archives.

890 **Appendix C.** Land cover types based on CORINE datasets, CNRS vegetation map and local maps

891 from Houet et al. (2012), and their absolute proportions of the 20 taxa.

892

Appendix A. POLLSCAPE simulation and evaluation of the Landscape Reconstruction Algorithm for mountain regions

A-1. POLLSCAPE simulations (Sugita 1994, 2013; Sugita et al., 1999; Gaillard et al., 2008) and parameter setting

POLLSCAPE is a simple simulation approach to evaluate factors and mechanisms that affect pollen-vegetation relationships in patchy and heterogeneous landscapes (Sugita, 1994, 2013). Effects on pollen assemblages of various combinations of specific assumptions and conditions can be assessed; those factors include inter-taxonomic differences in productivity and fall speed of pollen, basin size, spatial patterns of plant distribution and land cover, and atmospheric conditions (e.g., wind speed and turbulence that simultaneously influence pollen dispersal and deposition). This modeling approach has been informative to provide plausible scenarios about how pollen assemblages from lakes and mires would reflect the surrounding vegetation (e.g., Sugita et al., 1997, 1999; Bunting et al., 2004; Bunting and Middleton, 2009; Caseldine et al., 2008; Fyfe, 2006; Gaillard et al., 2008; Hellman et al., 2008; Hjelle and Sugita, 2012).

Major basic assumptions and conditions of the POLLSCAPE approach in this study are as follows:

- The sampling basin, either a lake or mire, is a circular opening in the vegetation canopy on a flat two-dimensional plain; heights of source plants for pollen are assumed to be at the ground level.
- Each taxon has a constant pollen productivity in the entire simulated plot.
- Wind above canopy is the dominant agent of pollen transport.
- Wind direction is even in all directions. Accordingly the spatial distribution of source plants for each taxon is described as a function of distance from a point at the center of the basin.
- Pollen dispersal is approximated either by a Gaussian Plume Model (GPM) of small particles from a ground-level source under various atmospheric conditions (Sutton, 1953; Tauber ,1965; Prentice, 1985, 1988; Sugita, 1993, 1994) or by a Lagrangian Stochastic Model (LSM) under more realistic wind-fields and atmospheric turbulence conditions (Kuparinen et al., 2007; Theuerkauf et al., 2016).
- When pollen assemblages from lakes are concerned, Sugita's model (Sugita, 1993) is used for approximation of pollen deposition on the entire lake surface either by the GPM or the LSM.

For the sake of simplicity this simulation study assumes mountain tops and high plateaus as “landscape islands” on a flat two-dimensional terrain 80 km x 80 km in size. Wind fields and turbulence in mountain regions are complex in reality; thus, pollen transport is area- and region-

specific, making it hard to model in a general way. Although the simulated plots with flat terrains are simplistic, it captures the main characteristics of the spatial structure and species composition of plant communities both in high plateaus and the regional vegetation around the Vicdessos valley (Figure 1a in the main text).

Table A-1 shows the parameter setting for the simulated landscapes, including the mean plant composition in proportion for individual patch types and the matrix in 80 km x 80 km plots. The Matrix and Patch Type B represent plant communities in lower altitudes including mountain valleys and flat plains. The Matrix is characterized by forests consisted of broadleaved and conifer trees (*Fagus*, *Quercus* and *Pinus*) with small amounts of grasses (Poaceae) and Ericaceous plants (*Calluna* and other Ericaceae taxa). Patch type B represents Poaceae-dominated unforested/open areas. Patch Type A symbolizes mountain tops that are characterized by Ericaceae plants (including *Rhododendron spp.* and *Vaccinium spp.*) with semi-dominant grass and *Calluna* (heather). Within the areas occupied by Patch Type A, small-patches of two types of heather heathlands are placed to create a localized mosaic of mountain plant communities: Patch Type C with heather, grass and Ericaceae and Patch Type D with heather, grass, Ericaceae and *Pinus*. Patch Type A occupies 30% of the total area in the 80-km x 80-km plots, and the Matrix and Patch Type B 50% and 20%, respectively. Within the "mountain" areas covered by Patch Type A, Patch Types C and D occupy 20% and 10% in area respectively; the rest (i.e. 70% in mountain area) is characterized by plant composition of Patch Type A. For all the patch types circular-shaped patches are placed randomly without overlap; patch sizes (±SE) for Patch Types A, B, C and D are 314 (±15) ha, 10 (±1) ha, 2 (±0.2) ha and 1 (±0.1) ha, respectively.

Simulations place different-sized and circular-shaped lakes - 500 m and 50 m in radius - only in patches of Patch Type A. Pollen data from 500-m radius lakes are used for REVEALS modeling in the LRA (Sugita, 2007a) to estimate the mean vegetation composition within a 100-km radius from the center of individual lakes; those from 50-m radius lakes are applied for LOVE modeling (Sugita, 2007b) to evaluate the relevant source area of pollen (RSAP; *sensu* Sugita, 1994) and estimate the local vegetation composition within the RSAP. A 500-m radius lake is set at the center of a patch of Patch Type A that is randomly selected in the central part of the plot; we repeat the same process thirty times to obtain thirty sets of pollen loading and proportions independently. For a 50-m radius lake the same sampling scheme is used, except for the location of the lake that is placed randomly within a patch of Patch Type A; then we repeat the process thirty times. Each trial, either for a 500-m radius lake or a 50-m radius lake, is run independently from the other runs. Mean plant abundance (i.e. the area occupied by each plant type per unit area) is calculated in consecutive concentric rings 5-m in width from the lake shore out to 100 km. For plant abundance data beyond the 80 km x 80 km plot border, simulations assume the outside-plot vegetation as homogeneous and the plant composition the same as that within the plot for the constituent taxa (the last column in

Table A-1).

Table A-1. Parameter setting for simulated landscapes

					Nested patches within Patch Type A		
		Matrix	Patch Type A	Patch Type B	Patch Type C	Patch Type D	
Landscape design	Areal proportion	0.50	0.30	0.20	0.20	0.10	
	Patch size (±SE) in ha		314±15	10±1	2±0.2	1±0.1	
							Overall proportion in the entire plot
Plant composition in each patch type and the matrix	Poaceae	0.03	0.15	0.94	0.21	0.30	0.256
	Pinus	0.40	0.02	0.01	0.01	0.05	0.208
	Betula	0.05	0.01	0.01	0.01	0.01	0.030
	Quercus	0.30	0.01	0.01	0.01	0.01	0.155
	Fagus	0.20	0.01	0.01	0.01	0.01	0.105
	Calluna	0.01	0.10	0.01	0.55	0.40	0.073
	Ericaceae	0.01	0.70	0.01	0.20	0.22	0.173
	SUM	1.00	1.00	1.00	1.00	1.00	1.000

Pollen dispersal and deposition is modeled by both the GPM and LSM options implemented in POLLSCAPE2017.v3.4.exe (Sugita, unpublished). The LSM option uses a look-up table of distance-dependent pollen deposition from a single point source based on the LSM model of Kuparinen et al. (2007) and Theuerkauf et al. (2016); the table was obtained from M. Theuerkauf. This implementation assumes the pollen source area to be within a 100-km radius from each lake. The GPM option, based on Sutton (1953), has been applied in palynology since the 1960s (Tauber, 1965). Those dispersal models are used to obtain the distance-weighted plant abundance (DWPA) of the surrounding vegetation, using the mean plant-abundance data at every 5-m increment out to 100 km at each site. In theory, pollen loading is linearly related to the DWPA for each of the constituent plant taxa (Prentice, 1985; Sugita, 1993, 1994, 2007a, 2007b); the slope of the relationship represents pollen productivity of the corresponding taxon. Pollen productivity estimates (PPEs) relative to that of Poaceae are listed in Table A-2 (after Mazier et al., 2012). Those estimates were compiled from previous studies in various parts of northwestern Europe (Broström et al., 2008; many others). Those studies cited use the Extended R-Value (ERV) model for obtaining PPEs, assuming that pollen dispersal and deposition follows the GPM (Prentice, 1985; Sugita, 1994). With the LSM option the

number of European plant/pollen types, for which PPEs are available, is still limited, except for PPEs obtained in Theuerkauf et al. (2013). This study uses the estimates in Table A-2 as inputs to simulation runs with either the GPM or the LSM, for the sake of consistency. Table A-2 also includes estimates of the fall speed of pollen in air - an important parameter for either the GPM or the LSM - for individual taxa (after Mazier et al., 2012).

Table A-2. Relative pollen productivity and fall speed of pollen used in simulations (after Mazier et al., 2012)

	Relative pollen productivity	Fall speed of pollen [m sec^{-1}]
Poaceae	1.00	0.035
Pinus	6.38	0.031
Betula	3.09	0.024
Quercus	5.83	0.035
Fagus	2.35	0.057
Calluna	0.82	0.038
Ericaceae	0.07	0.038

POLLSCAPE simulations result in pollen proportions of the constituent taxa at each lake, calculated from the pollen loading data relative to that of a reference taxon. Pollen counts are then obtained by back calculation in such a way that the total sum becomes 1000 grains at each site.

A-2. Landscape Reconstruction Algorithm (LRA – Sugita, 2007a, 2007b; Sugita et al., 2010)

The Landscape Reconstruction Algorithm (LRA) consists of two steps: estimating regional vegetation using the REVEALS model (Sugita, 2007a) and local vegetation using the LOVE model (Sugita, 2007b). REVEALS outcomes provide the mean vegetation composition, not distance weighted, within a 50-100 km radius. With the REVEALS results as inputs, LOVE calculates the local vegetation composition in a distance-weighted fashion within the relevant source area of pollen (RSAP) - the smallest spatial scale possible for local vegetation reconstruction (Sugita, 1994, 2007b; Sugita et al., 2010). Both the GPM and the LSM options are used for the LRA applications for comparison. Relative PPEs and fall speed of pollen in Table A-2 are entered to all the LRA runs.

All the LOVE-based estimates of local vegetation within the RSAP are obtained using pollen data from lake 50-m in radius. An inverse modeling approach of LOVE (Sugita, 2007b; Sugita

et al., 2010) is applied for the RSAP estimate for all the LRA runs. The basic assumptions and conditions described in the POLLSCAPE section above are mostly the same for the Landscape Reconstruction Algorithm (LRA) applied in the simulation runs here.

Ideally pollen records from large sites >100 ha are preferable for REVEALS applications (Sugita, 2007a). The main conclusions of this simulation study (i.e. Figure 1 in the main text) are drawn from the result based on the REVEALS runs with pollen data from 500-m radius lakes. When large sites are unavailable as in most mountain regions, pollen records from a number of small sites could potentially be used for both the REVEALS and LOVE applications; however, uncertainties of the regional vegetation estimates in particular are expected to increase in unknown ways (Sugita, 2007a; Sugita et al., 2010; Fyfe et al., 2013; Mazier et al., 2015; Trondman et al., 2016).

To evaluate uncertainties and accuracy of the LRA results when pollen records from small sites are used for REVEALS in mountain situations, we conducted additional simulation runs, assuming that the REVEALS estimates of regional vegetation composition are obtained using pollen records from 50-m radius lakes (i.e. those are the same as those created for the LOVE calculations in the main simulation runs). Figure A-1 shows the simulation result.

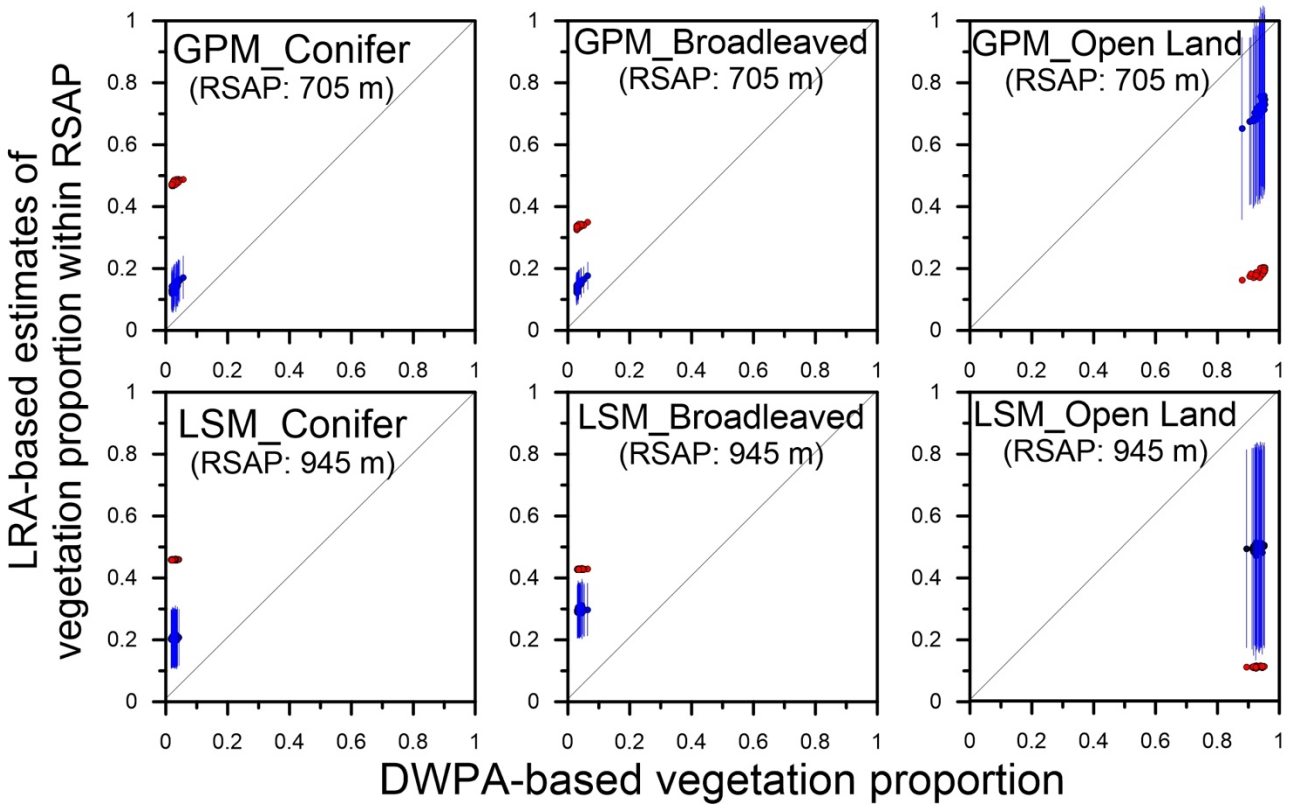

Figure A-1. LRA-based estimates of local vegetation against DWPA-based vegetation proportion within RSAP, assuming all the pollen records are from 50-m radius lakes in Patch Type A. Blue dots and error bars indicate the LRA estimates and their SEs against vegetation proportions at 30 sites; red dots represent pollen proportions at 30 sites. RSAP is the area within a 705-m radius when GPM is used and within a 945-m radius when LSM is used.

When all pollen sites are small lakes 50-m in radius for both the REVEALS and LOVE runs, the accuracy of the LRA results are not as good as those shown in Figure 1-b in the main text. The RSAP estimates become larger than those shown in Figure 1-b: 705 m (GPM) and 945 m (LSM) against 310 m (GPM) and 325 m (LSM). Although Figure A-1 indicate that the LRA still improves significantly the accuracy of vegetation reconstruction over pollen percentages alone, the simulation results demonstrate that regional vegetation reconstruction using pollen records from "large sites" is preferred whenever possible to reduce impacts on the LRA results and reliability of the systematic selection of pollen sites only on mountain tops (Sugita, 2007a).

REFERENCES

Broström, A., Nielsen, A.B., Gaillard, M.J. et al. (2008) Pollen productivity estimates of key European plant taxa for quantitative reconstruction of past vegetation: a review. Vegetation History and Archaeobotany, 17, 461-478.

Bunting, M.J. & Middleton, R. (2009) Equifinality and uncertainty in the interpretation of pollen data: the Multiple Scenario Approach to reconstruction of past vegetation mosaics. The Holocene, 19, 799-803.

Bunting, M.J., Gaillard, M.J., Sugita, S. et al. (2004) Vegetation structure and pollen source area. The Holocene, 14, 651-660.

Caseldine, C., Fyfe, R.M., Hjelle, K. (2008) Pollen modelling, palaeoecology and archaeology: virtualization and/or visualisation of the past? Vegetation History and Archaeobotany, 17, 543-549.

Fyfe, R.M. (2006) GIS and the application of a model of pollen deposition and dispersal: A new approach to testing landscape hypotheses using the POLLANDCAL models. Journal of Archaeological Science, 33, 483-493.

Fyfe, R.M., Twiddle, C., Sugita, S. et al. (2013) The Holocene vegetation cover of Britain and Ireland: overcoming problems of scale and discerning patterns of openness. Quaternary Science Reviews, 73, 132-148.

Gaillard, M.J., Sugita, S., Bunting, M.J. et al. (2008) The use of modelling and simulation approach in reconstructing past landscapes from fossil pollen data: a review and results from the POLLANDCAL network. Vegetation History and Archaeobotany, 17, 419-443.

Hellman, S., Gaillard, M.J., Broström, A. & Sugita, S. (2008) Effects of the sampling design and selection of parameter values on pollen-based quantitative reconstructions of regional vegetation: a case study in southern Sweden using the REVEALS model. Vegetation History and

Archaeobotany, 17, 445-459.

Hjelle, K.L. & Sugita, S. (2012) Estimating pollen productivity and relevant source area of pollen using lake sediments in Norway: how does lake size variation affect the estimates? The Holocene, 22, 313-324.

Kuparinen, A., Markkanen, T., Riikonen, H. et al. (2007) Modeling air-mediated dispersal of spores, pollen and seeds in forested areas. Ecological Modelling, 208, 177-188.

Mazier, F., Gaillard, M.J., Kuneš, P. et al. (2012) Testing the effect of site selection and parameter setting on REVEALS-model estimates of plant abundance using the Czech Quaternary Palynological Database. Review of Palaeobotany and Palynology, 187, 38-49.

Mazier, F., Broström, A., Bragée, P. et al. (2015) Two hundred years of land-use change in the South Swedish Uplands: comparison of historical map-based estimates with a pollen-based reconstruction using the landscape reconstruction algorithm. Vegetation History and Archaeobotany, 24, 555-570.

Prentice, I.C. (1985) Pollen representation, source area, and basin size: toward a unified theory of pollen analysis. Quaternary Research, 23,76-86.

Prentice, I.C. (1988) Records of vegetation in time and space: the principles of pollen analysis. In: Huntley, B. & Webb, T. (Eds.) Vegetation history. Kluwer, Dordrecht, pp. 17-42.

Sugita, S. (1993) A model of pollen source area for an entire lake surface. Quaternary Research, 39, 239-244.

Sugita, S. (1994) Pollen representation of vegetation in Quaternary sediments: Theory and method in patchy vegetation. Journal of Ecology, 82, 881-897.

Sugita, S. (2007a) Theory of quantitative reconstruction of vegetation I: Pollen from large sites REVEALS regional vegetation composition. The Holocene, 17, 229-241.

Sugita, S. (2007b) Theory of quantitative reconstruction of vegetation II: All you need is LOVE. The Holocene, 17, 243-257.

Sugita, S. (2013) Pollen methods and studies, POLLSCAPE Model: Simulation Approach for Pollen Representation of Vegetation and Land Cover. In: Scott A. Elias (Ed) Encyclopedia of Quaternary Science (Second Edition). Elsevier, Amsterdam, pp. 871-879.

Sugita, S., MacDonald, G.M. & Larsen, C.P.S. (1997) Reconstruction of fire disturbance and forest succession from fossil pollen in lake sediments: potential and limitations. In: Clark, J.S., Cachier, H. et al. (Eds.) Sediment Records of Biomass Burning and Global Change. Springer, Berlin, pp. 387-412.

Sugita, S., Gaillard, M.J. & Broström, A. (1999) Landscape openness and pollen records: a simulation approach. The Holocene, 9, 409-421.

Sugita, S., Hicks, S. & Sormunen, H. (2010) Absolute pollen productivity and pollen-vegetation relationships in northern Finland. Journal of Quaternary Science, 25, 724-736.

Sutton, O.G. (1953) Micrometeorology. McGraw-Hill.

Tauber, H. (1965) Differential pollen dispersion and the interpretation of pollen diagrams. Danmarks Geologiske Undersøgelse. II. RÆKKE, No. 89: 1-69.

Theuerkauf, M., Kuparinen, A. & Joosten, H. (2013) Pollen productivity estimates strongly depend on assumed pollen dispersal. The Holocene, 23, 14-24.

Theuerkauf, M., Couwenberg, J., Kuparinen, A. et al. (2016) A matter of dispersal: REVEALSinR introduces state-of-the-art dispersal models to quantitative vegetation reconstruction. Vegetation History and Archaeobotany, 25, 541-553.

Trondman, A.K., Gaillard, M.J., Sugita, S. et al. (2016) Are pollen records from small sites appropriate for REVEALS model-based quantitative reconstructions of past regional vegetation? An empirical test in southern Sweden. Vegetation History and Archaeobotany, 25, 131-151.

Appendix B. Dated materials and details on age-depth models of sedimentary archives.

Lake and peat cores were dated by using radiocarbon and ^{210}Pb ages together. Age-depth models were based on all available age dating information and the entire cores, although the present study focused on the last 60 years. Radiocarbon dating were obtained from previously-identified above-ground plant remains selected from 1 cm^3 of bulk peat/sediment at EcoLab and GEODE laboratories following Mauquoy et al. (2004). Sample pretreatments included acid-alkali-acid washing (to remove bacterial CO_2, carbonate and humic-fulvic acids), drying, combustion and graphitization. These pretreatments and the radiocarbon measurements by acceleration mass spectrometer were performed at Beta Analytic (London, UK), Poznan Radiocarbon Laboratory (Poznan, Poland) and ARTEMIS facility (CNRS-Gif sur Yvette, France). ^{210}Pb measurements were achieved by using peat powder and Gamma spectrometry (Van Beek et al., 2013; Appleby, 2002), except Orry de Théo peatland for which Alpha spectrometry was used (Sanchez-Cabeza et al., 1998).

Table B-1 summarizes the dating information. The age-depth models of Legunabens, Arbu and Fouzes that were not published so far are given below.

Table B-1. Background information about the dating used in this study.

Site name	Type of Records	^{14}C Bomb Pulse	^{210}Pb	Number of ^{14}C ages	References
Sigriou (SIG)	Lake		Gamma spec.	n=5 (+ 2 outliers)	Simonneau et al. 2013
Legunabens (LEG)	Lake	2		3	this study
Arbu (ARBU)	Lake		Gamma spec.	3	this study
Escale (ESC)	Peat		Gamma spec.	2	Hansson et al. 2017
Fouzes (FOUZ)	Peat		Gamma spec.	0	this study
W1652a (W1652)	Peat	5	Gamma spec.	4	Hansson et al. 2017
Etang mort (EM)	Peat		Gamma spec.	2	Hansson et al. 2017
Orry de Théo (OT)	Peat		Alpha spec.	4	Galop et al. 2011

LEGUNABENS

The age-depth model of Legunabens sediment core is based on five radiocarbon measurements from macrofossils. Three radiocarbon ages are calibrated by using the NH IntCal09 calibration curve. The results from the two upper sediment layers are used as post-bomb ages (Goodsite et al., 2001). The Clam age-depth model is shown in figures B-1 and B-2 and all details about radiocarbon measurements are described in Table B-2 below.

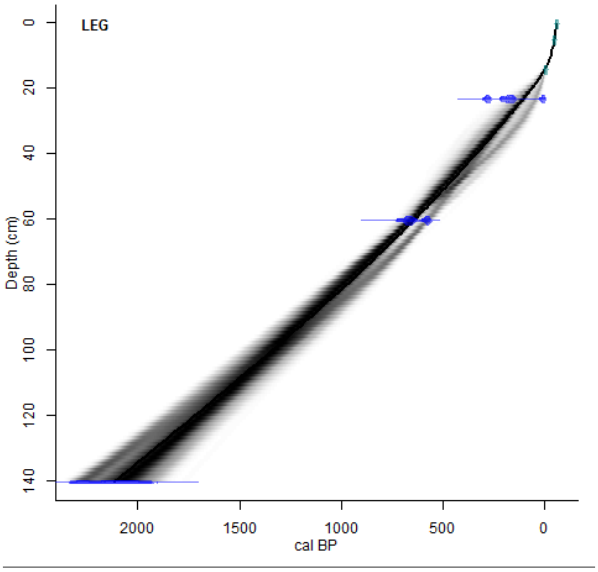

Figure B-1. Clam age-depth model for Legunabens.

Table B-2. Background information about the dating used for Legunabens.

Legunabens Raw radiocarbon measurements	Mass in grams	Laboratory label and type of macrofossils that has been dated		^{14}C uncal.
LG01 05-06	5.5	Poz-49543	Sphagnum leaves and branches, + insect remains	105.7 ± 1.08 pMC
LG01 14-15	14.5	Poz-49578	Sphagnum leaves and branches, + insect remains	113.86 ± 1.23 pMC
LG01 23-24 CS	23.5	Poz-49576	Sphagnum leaves and branches, + other mosses sp.	195 ± 30
LG01 60-61 CS	60.5	Poz-49575	Sphagnum leaves and branches, and some insect remains	700 ± 50
LG01 140-141 CS	140.5	Poz-49542	Leaves of Sphagnum sp.	2130 ± 90

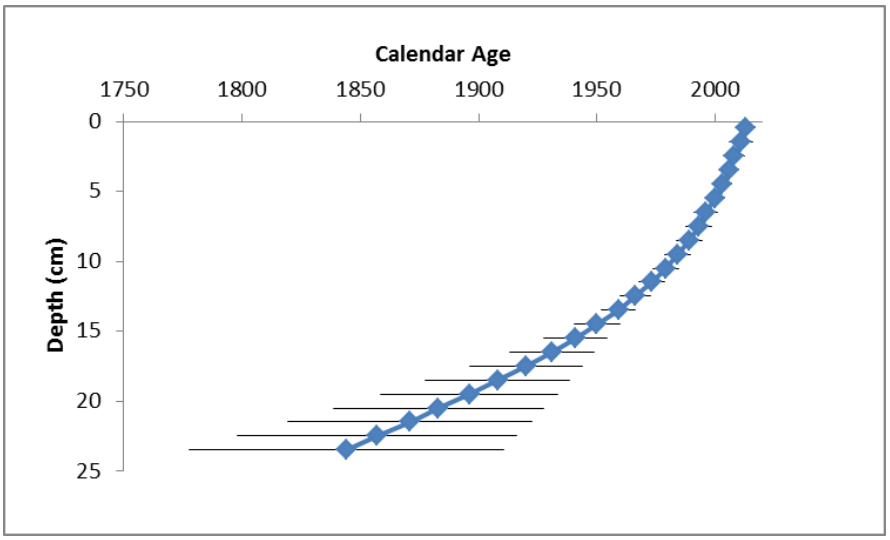

Figure B-2. Zoom on the outcomes of the Clam age-depth model for the upper sediment layers of Legunabens.

FOUZES

^{210}Pb and other radionuclides were measured at LAFARA/OMP by gamma Spectrometry (P. Van Beek and M. Souhault) - https://lafara.obs-mip.fr/. Unsupported ^{210}Pb was estimated using total ^{210}Pb and ^{226}Ra (^{214}Pb) to assess supported ^{210}Pb. Age dating was estimated using the CRS model (Appleby, 2002) and model uncertainties were calculated with MonteCarlo simulations (Binford et al., 1990) based on a Matlab routine written by P.E. Higuera and modified by M. Enrico. The age-depth model was validated by the measurements of a ^{137}Cs peak around 1960 and the detection of ^{241}Am traces at the same time period. The Clam age-depth model is shown in Figure B-3.

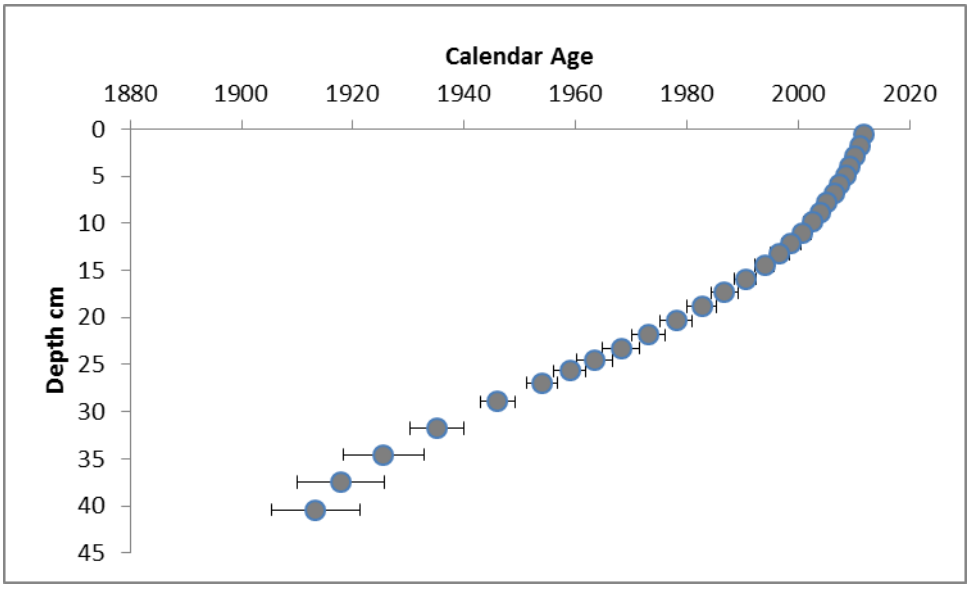

Figure B-3. Clam age-depth model for Fouzes.

ARBU

The age-depth model for Arbu sedimentary core is based on a combination of ^{210}Pb measurements (CRS model; Appleby, 2002) and three radiocarbon age dates. No ^{137}Cs peak was clearly defined, however ^{137}Cs was found in the layer dated after 1950 with an increase until ~1960. A clear peak of ^{241}Am was found for the sediment slices dated from 1955 to 1975. The Clam age-depth model is shown in Figure B-4. Figure B-5 corresponds to a zoom on the outcomes of the Clam age-depth model for the upper sediment layers.

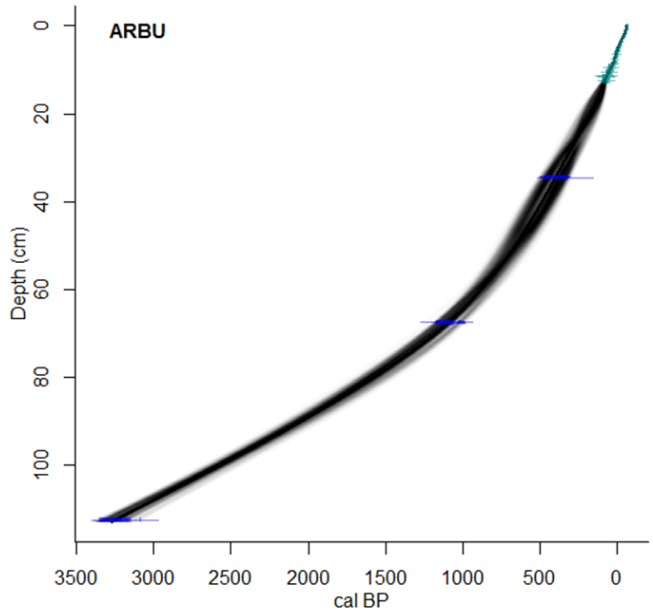

Figure B-1. Clam age-depth model for Arbu.

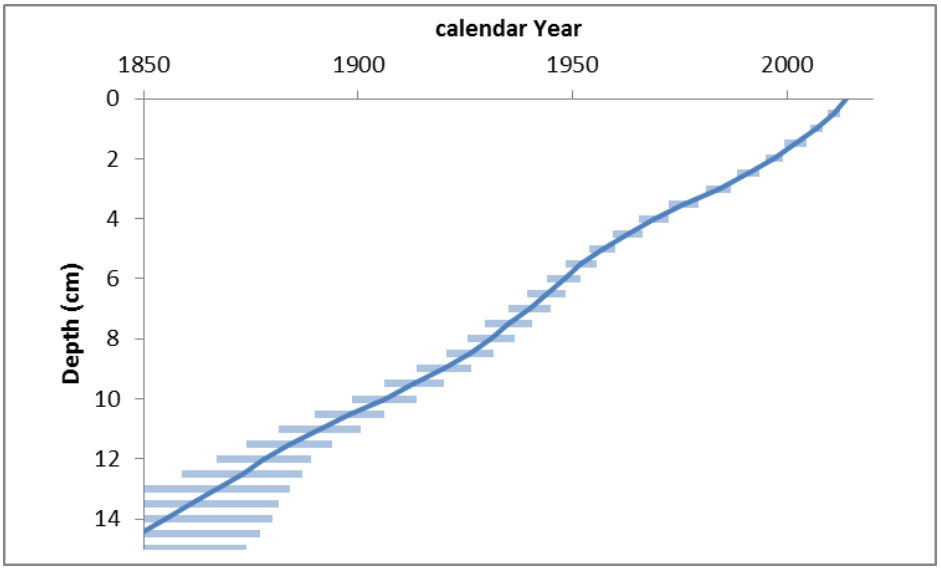

Figure B-2. Zoom on the outcomes of the Clam age-depth model for the upper sediment layers of Arbu.

REFERENCES

Appleby, P.G. (2002) Chronostratigraphic techniques in recent sediments. In: Tracking environmental change using lake sediments. Springer, Dordrecht, p. 171-203.

van Beek, P., Souhaut, M., Lansard, B. et al. (2013) LAFARA: A new underground laboratory in the French Pyrénées for low-background gamma spectrometry. Journal of Environmental Radioactivity, 116, 152-158.

Galop, D., Houet, T., Mazier, F. et al. (2011) Grazing activities and biodiversity history in the Pyrenees: New insights on high altitude ecosystems in the framework of a Human-Environment Observatory. Past Global Changes Magazine, 19, 53-55.

Goodsite, M.E., Rom, W., Heinemeier, J. et al. (2001) High-resolution AMS 14 C dating of post-bomb peat archives of atmospheric pollutants. Radiocarbon, 43, 495-515.

Hansson, S.V., Claustres, A., Probst, A. et al. (2017) Atmospheric and terrigenous metal accumulation over 3000 years in a French mountain catchment: Local vs distal influences. Anthropocene, 19, 45-54.

Mauquoy, D., Blaauw, M., van Geel, B. et al. (2004) Late Holocene climatic changes in Tierra del Fuego based on multiproxy analyses of peat deposits. Quaternary Research, 61, 148-158.

Sanchez-Cabeza, J.A., Masqué, P. & Ani-Ragolta, I. (1998) ^{210}Pb and ^{210}Po analysis in sediments and soils by microwave acid digestion. Journal of Radioanalytical and Nuclear Chemistry, 227, 19-22.

Simonneau, A., Chapron, E., Courp, T. et al. (2013) Recent climatic and anthropogenic imprints on lacustrine systems in the Pyrenean Mountains inferred from minerogenic and organic clastic supply (Vicdessos valley, Pyrenees, France). The Holocene, 23, 1762-1775.

MAX-PLANCK-INSTITUT FÜR CHEMIE
MAX-PLANCK-GESELLSCHAFT

Dr. Laurent Marquer
Research Group for Terrestrial Palaeoclimates
Max Planck Institute for Chemistry, Mainz (Germany)
E-mails: laurent.marquer.es@gmail.com; l.marquer@mpic.de

To: J. S. Carrion (Editor of *Quaternary Science Reviews*).

Mainz, October 24th 2019

Dear Professor Carrion,

We have no conflict of interest to declare.

Yours sincerely,

Laurent Marquer and the co-authors.

Author contributions

L.M., F.M, S.S. and M.J.G. conceived the initial idea; L.M. ran the LRA model; S.S. led the runs related to the evaluation with simulated landscapes; D.G., F.M. and E.F. provided the pollen data; T.H. provided the local land-cover maps for three time windows; S.H. and N.D.M. provided the plant composition in each land-cover type; A.S., F.D.V. and G.L.R. provided the age-depth models at individual sites. L.M. led analyses and writing with substantial input from F.M. and S.S. All authors contributed to various versions of the manuscript.